

Small Instanton Effects on Composite Axion Mass

Takafumi Aoki^a, Masahiro Ibe^{a,b}, Satoshi Shirai^b, and Keiichi Watanabe^a

^a *ICRR, The University of Tokyo, Kashiwa, Chiba 277-8582, Japan*

^b *Kavli Institute for the Physics and Mathematics of the Universe (WPI),
The University of Tokyo Institutes for Advanced Study,
The University of Tokyo, Kashiwa 277-8583, Japan*

Abstract

This paper investigates the impact of small instanton effects on the axion mass in composite axion models. In particular, we focus on the Composite Accidental Axion (CAA) models, which are designed to address the axion quality problem, and where the Peccei-Quinn (PQ) symmetry emerges accidentally. In the CAA models, the QCD gauge symmetry is embedded in a larger gauge group at high energy. These models contain small instantons not included in low-energy QCD, which could enhance the axion mass significantly. However, in the CAA models, our analysis reveals that these effects on the axion mass are non-vanishing but are negligible compared to the QCD effects. The suppression of the small instanton effects originates from the global chiral $U(1)$ symmetries which are not broken spontaneously and play a crucial role in eliminating θ -terms in the hidden sectors through anomalies. We find these $U(1)$ symmetries restrict the impact of small instantons in hidden sectors on the axion mass. Our study provides crucial insights into the dynamics within the CAA models and suggests broader implications for understanding small instanton effects in other composite axion models.

Contents

1	Introduction	1
2	Small Instanton Effects on Axion Mass without Fermion	3
2.1	Constrained Instanton	3
2.2	Axion Mass Enhancement in Model without Fermion	4
3	Model of Composite Accidental Axion	6
3.1	Composite Axion Model	6
3.2	$SU(3) \times SU(N)^{n_s} \times SU(4)^{n_s-1}$ Model	7
4	Small Instanton Effects vs Chiral Symmetry	11
4.1	Toy Example: $SU(3)_w \times SU(4)_w$ Model	11
4.2	Suppression of Instanton Effects by Anomalous Symmetry	12
4.3	Fermion Zero Modes and 't Hooft Operator	13
4.4	Non-vanishing Small Instanton Effects in $SU(3)_w \times SU(4)_w$ model	15
5	Small Instanton Effects on Composite Accidental Axion	20
5.1	Vanishing Small Instanton Effects	20
5.2	Non-vanishing Small Instanton Effects	21
5.3	Small Instanton Effects for $n_s > 2$	23
6	Application to Other Composite Axion Models	23
6.1	Composite Axion Models with Spectator QCD	23
6.2	Axial $SU(3) \times [SU(N)]^{n'_s} \times [SU(m)]^{n'_s}$ Model	24
7	Conclusions	25
A	Notation and Remarks on Euclidean Space	27
A.1	Notation in Euclidean Space	27
A.2	Remarks on Fermions in Euclidean Space	28
B	Zero Modes of Massive Fermions around Constrained Instanton	28

1 Introduction

The Peccei-Quinn (PQ) mechanism is the most prominent solution to the strong CP problem [1–4]. In this mechanism, a global U(1) symmetry called PQ symmetry, plays a crucial role. This symmetry is an exact symmetry, except for the axial anomaly of QCD. With the spontaneous symmetry breaking (SSB) of PQ symmetry, the effective θ -angle of QCD is cancelled by the vacuum expectation value (VEV) of the axion, so that the strong CP problem is solved.

However, the assumption of such a convenient global symmetry seems to be weakly grounded. By its definition, the PQ symmetry is an inexact symmetry due to the anomaly. It is also argued that all global symmetries are broken by quantum gravity effects [5–10]. These arguments suggest that the presence of (higher-dimensional) operators that violate the PQ symmetry cannot generally

be ruled out. When such operators are present, the resultant effective θ -angle easily exceeds the experimental constraints, and spoils the PQ mechanism [10–12]. This issue is known as the axion quality problem.

The axion quality problem has motivated various extensions of axion models, so that a PQ symmetry emerges as an almost exact symmetry. For instance, the accidental PQ symmetry can be achieved by certain (discrete) gauge symmetries, as detailed in Refs. [12–23]. Alternatively, a high-quality PQ symmetry may arise from an extra-dimensional setup [24–30]. In this paper, we focus on composite axion models with high-quality accidental PQ symmetry.

The composite axion model has been proposed to solve another problem of the invisible axion model, i.e., the fine-tuning problem of the axion decay constant. In the invisible axion model, the astrophysical constraints and dark matter abundance imply the axion decay constant f_a in the range of $f_a = \mathcal{O}(10^{8-12})$ GeV (see e.g. Ref. [31]), which requires fine-tuning. The composite axion model resolves this issue by achieving the intermediate scale through hidden strongly-coupled gauge dynamics via dimensional transmutation [32, 33]. This hidden gauge interaction, referred to as “axicolor,” confines fermions charged under it, resulting in the axion as a composite state.

In addition to solving the fine-tuning problem, composite axion models are advantageous in achieving high-quality PQ symmetry as an accidental global symmetry of the axicolor fermions. Several composite axion models have been proposed to address the axion quality problem [34–41].

In many axion models with high-quality PQ symmetry, $SU(3)_{\text{QCD}}$ is embedded in a larger gauge group. In such cases, the axion can couple to the larger gauge group, in addition to $SU(3)_{\text{QCD}}$. Such dynamics can affect the axion potential, possibly spoiling the PQ mechanism due to the θ -terms in hidden sectors or modifying the prediction of the axion mass. Therefore, in extended axion models, effects on the axion potential from these new interactions must be examined.

Among the possible effects from these new interactions, instanton configurations not present in QCD can significantly impact the axion potential. These configurations are often called small instantons. In fact, Ref. [42] pointed out that small instanton effects from new gauge interactions can enhance the axion mass in some models. The small instanton effects are currently subjects of intense interest and debate in the field [43–48].

In this paper, we discuss small instanton effects on the axion mass in composite axion models with high-quality PQ symmetry. In particular, we mainly focus on Composite Accidental Axion (CAA) models, proposed by Redi and Sato [36]. One advantageous feature of the CAA models is that the alignment of the effective QCD θ -angle to 0 is protected by symmetries. Specifically, symmetries which are anomalous but not broken spontaneously eliminate θ -angles in hidden sectors (see Sec. 3). However, it is still unclear whether small instanton effects impact the axion mass, and if they do, to what extent they have an impact.

If the mass of the axion is enhanced, it has substantial theoretical and phenomenological implications. Theoretically, an increase in axion mass can mitigate the axion quality problem. Phenomenologically, a higher axion mass significantly impacts accelerator experiments and astrophysical constraints. For instance, a sufficiently large axion mass can relax experimental and observational constraints, allowing for a smaller decay constant f_a , which further alleviates the axion quality problem [49]. Therefore, a detailed study of the axion mass is highly important.

As we will see, small instantons in the CAA models do contribute to the axion mass, in addition to the QCD contributions. We will also find, however, that those contributions are negligibly small compared with the QCD contributions. To derive these conclusions, accidental chiral $U(1)$ symmetries other than the PQ symmetry, which are responsible for eliminating θ -terms in hidden

sectors, play a crucial role. As discussed in Sec. 4, the suppression of small instanton effects on the axion mass stems from the fact that the PQ symmetry is not unique but can be redefined as a linear combination with the U(1) symmetries. Our conclusion is not limited to the CAA models but is applicable to a wide range of axion models with high-quality PQ symmetry. It highlights the challenge of enhancing the axion mass without spoiling the high-quality PQ symmetry.

The organization of this paper is as follows. In Sec. 2, we briefly review the small instanton effects on the axion potential, in a simple model without fermions. In Sec. 3, we review the composite axion model in Refs. [32, 33] and the simplest CAA model. In Sec. 4, we discuss small instanton effects in a perturbative toy model mimicking the CAA model. In Sec. 5, we discuss the small instanton effects in the CAA model. In Sec. 6, we also discuss other composite axion models. The final section is devoted to our conclusions.

2 Small Instanton Effects on Axion Mass without Fermion

In the CAA models, the accidental PQ symmetry is spontaneously broken due to the axicolor dynamics. This dynamics also breaks a product gauge group, resulting in $SU(3)_{\text{QCD}}$ emerging as an unbroken diagonal subgroup. In this section, we review a model where small instantons not included in low-energy QCD enhance the axion mass significantly [42, 44].

2.1 Constrained Instanton

We consider a model where the small instantons which are not included in the low-energy QCD reside in a broken part of the product gauge group. Instanton configurations in the broken phase are called constrained instanton [50]. The essential points of the constrained instantons can be understood by considering a spontaneously broken $SU(2)$ gauge theory as an example.

Following Ref. [51], we assume $SU(2)$ gauge symmetry is broken by the VEV of an $SU(2)$ doublet scalar field H . The Euclidean Lagrangian of this system is given by,¹

$$\mathcal{L}_E = \frac{1}{2g^2} \text{Tr}(F_{\mu\nu}F_{\mu\nu}) + (D_\mu H)^\dagger (D_\mu H) + \frac{\lambda}{4} (H^\dagger H - v^2)^2, \quad (2.1)$$

where the field strength and the covariant derivatives are defined by

$$\begin{aligned} F_{\mu\nu} &= \partial_\mu A_\nu - \partial_\nu A_\mu - i[A_\mu, A_\nu], \\ D_\mu &= \partial_\mu - iA_\mu. \end{aligned}$$

See Appendix A for notations of Euclidean space. Here, g is the $SU(2)$ gauge coupling, $\lambda > 0$ is the quartic coupling, $v > 0$ is a mass dimensional parameter, and $A_\mu = A_\mu^a \tau^a / 2$ ($a = 1, 2, 3$) with τ^a being the Pauli matrices. At the vacuum, H obtains a VEV,

$$\langle H \rangle = \begin{pmatrix} 0 \\ v \end{pmatrix}, \quad (2.2)$$

which breaks $SU(2)$ completely. The physical scalar boson mass is given by $m_H = \sqrt{\lambda}v$ and the gauge boson mass is given by $m_A = gv/\sqrt{2}$.

¹We take the Euclidean metric to be $g_{\mu\nu} = (+, +, +, +)$

For $v = 0$, i.e., in the unbroken phase, instanton configurations are local minima of the Euclidean action, which are labeled by winding number w . An instanton configuration with $w = 1$ is given by,

$$A_\mu = \frac{2\rho^2 x_\nu}{x^2(x^2 + \rho^2)} \bar{\tau}_{\mu\nu} , \quad H = 0 , \quad (2.3)$$

where ρ is the instanton size and $\bar{\tau}_{\mu\nu}$ is defined in Eq. (A.9). In the semi-classical approximation, an instanton configuration contributes to the path integral, which is suppressed by a factor e^{-S_E} with $S_E = 8\pi^2/g^2$, which is independent of the size ρ .

In the broken phase, where $v \neq 0$, no instanton solutions exist in the strict sense as local minima of the Euclidean action. As discussed in Ref. [50], an instanton-like configuration, whose size is much smaller than the inverse of the symmetry breaking scale v^{-1} , contributes to the semi-classical approximation of the path integral, similar to the instantons in the unbroken phase. An instanton-like configuration with a fixed size is called constrained instanton.

The constrained instanton solution looks like instanton for $x \ll m_{A,H}^{-1}$ while decaying exponentially at $x \gg m_{A,H}^{-1}$. At $x \ll m_{A,H}^{-1}$, the solution behaves as

$$A_\mu^{\text{inst}} = \frac{2\rho^2}{x^2(x^2 + \rho^2)} \bar{\tau}_{\mu\nu} x_\nu + \mathcal{O}((\rho m_{A,H})^2) , \quad (2.4)$$

$$H^{\text{inst}} = \left(\frac{x^2}{x^2 + \rho^2} \right)^{1/2} \begin{pmatrix} 0 \\ v \end{pmatrix} + \mathcal{O}((\rho m_{A,H})^2) . \quad (2.5)$$

Note that H has a nontrivial profile and SU(2) symmetry is restored at the origin. Similarly, we also obtain constrained anti-instanton solution by replacing $\bar{\tau}_{\mu\nu}$ with $\tau_{\mu\nu}$.

By substituting the constrained (anti-)instanton into the Euclidean action, we obtain,

$$S_E(\rho) = \frac{8\pi^2}{g^2} + \frac{4\pi^2 \rho^2 m_A^2}{g^2} + \frac{1}{g^2} \mathcal{O}(\rho^4 m_{A,H}^4) , \quad (2.6)$$

where the second term comes from the kinetic term of the scalar field, $|D_\mu H|^2$. Thus, for a sufficiently small constrained instanton i.e., $\rho m_{A,H} \ll 1$, it can play an important role in the semi-classical approximation as the (anti-)instanton configuration in the unbroken phase.

In this section, we have focused on an SU(2) gauge theory as a simple example. The insights gained about constrained instantons can be applicable to models that include larger gauge groups.

2.2 Axion Mass Enhancement in Model without Fermion

To see how the small instantons affect the axion potential, let us consider a model where $SU(3)_1 \times SU(3)_2$ is broken down to the diagonal subgroup $SU(3)_{\text{QCD}}$ [42]. We introduce two axions a_i ($i = 1, 2$) which couple to the $F\tilde{F}$ terms, i.e.

$$\mathcal{L} = \sum_{i=1}^2 \left[-\frac{1}{2g_i^2} \text{Tr}(F_i^{\mu\nu} F_{i\mu\nu}) + \frac{1}{16\pi^2} \left(\frac{a_i}{f_i} + \theta_i \right) \text{Tr}(F_i^{\mu\nu} \tilde{F}_{i\mu\nu}) \right] . \quad (2.7)$$

Here, $i = 1, 2$ denotes each gauge sector with the gauge coupling g_i and the vacuum angle θ_i . The domains of the axions are given by $a_i/f_i = [0, 2\pi)$, with f_i denoting the decay constants of the

axions. In this model, the PQ symmetries are realized as shifts of the axions, which are anomalous with respect to each $SU(3)_i$. In the presence of the two axions, both θ_1 and θ_2 can be set to zero by the shifts of the axions.

Let us assume that $SU(3)_1 \times SU(3)_2$ is broken down to $SU(3)_{\text{QCD}}$ by the VEV of a bi-fundamental $(\mathbf{3}, \bar{\mathbf{3}})$ scalar field, $\phi_c^{c'}$ ($c, c' = 1, 2, 3$), i.e.,

$$\langle \phi_c^{c'} \rangle = v \delta_c^{c'} . \quad (2.8)$$

We also assume that $SU(3)_1 \times SU(3)_2$ is weakly coupled at the scale around v . Below the breaking scale, the effective QCD coupling is given by,

$$\frac{1}{g_{\text{QCD}}^2(v)} = \frac{1}{g_1^2(v)} + \frac{1}{g_2^2(v)} , \quad (2.9)$$

where we take the renormalization scale $\mu = v$. The axions couple to QCD through

$$\mathcal{L} = -\frac{1}{2g_{\text{QCD}}^2} \text{Tr}(G^{\mu\nu} G_{\mu\nu}) + \frac{1}{16\pi^2} \left(\sum_i \frac{a_i}{f_i} \right) \text{Tr}(G^{\mu\nu} \tilde{G}_{\mu\nu}) , \quad (2.10)$$

where $G_{\mu\nu}$ denotes the field strength of QCD. Through this coupling, QCD contributes to the axion potential, which is roughly represented by the following expression:

$$V_{\text{QCD}}(a_1, a_2) \sim \Lambda_{\text{QCD}}^4 \cos \left(\sum_i \frac{a_i}{f_i} \right) . \quad (2.11)$$

Here, Λ_{QCD} is the dynamical scale of QCD.² The impact of quarks in the Standard Model (SM) on the axion potential will be discussed at the end of this section.

We denote the winding numbers of $SU(3)_1$ and $SU(3)_2$ sectors by k_1 and k_2 . Following Ref. [52], we label them by (k_1, k_2) . In the semi-classical approximation, the constrained instanton with a size ρ contributes to the path integral which is suppressed by $e^{-S_{\text{E}}}$ with the action,

$$S_{\text{E}i}(\rho) = \frac{8\pi^2}{g_i^2(\rho^{-1})} + \mathcal{O}(4\pi^2 \rho^2 v^2) , \quad (2.12)$$

where we consider either $(1, 0)$ or $(0, 1)$ instantons. Here, we have taken the renormalization scale of the gauge couplings to be the inverse of the small instanton size, $\mu = \rho^{-1}$ [53].

In this simple model, the small constrained instantons generate additional axion potentials, which are dominated by the contributions from those with $\rho \sim v^{-1}$. As a result, the total axion potential amounts to

$$V(a_1, a_2) \sim \Lambda_{\text{QCD}}^4 \cos \left(\sum_i \frac{a_i}{f_i} \right) + v^4 \sum_i e^{-\frac{8\pi^2}{g_i^2(v)}} \cos \left(\frac{a_i}{f_i} \right) . \quad (2.13)$$

²In the presence of light quarks, $V_{\text{QCD}} \simeq m_\pi^2 f_\pi^2 \cos(a/F_a)$, where m_π and f_π are the mass and the decay constant of the pion. Numerically $m_\pi^2 f_\pi^2 \sim \Lambda_{\text{QCD}}^4$. Therefore, for simplicity in the following discussion, we represent the low-energy QCD contributions to the axion potential using Λ_{QCD}^4 .

Since the dynamical scale of QCD is related to the symmetry breaking scale via

$$\Lambda_{\text{QCD}} = v e^{-\frac{1}{b_{\text{QCD}}} \frac{8\pi^2}{g_{\text{QCD}}^2(v)}}, \quad (2.14)$$

the axion potential can be rewritten as

$$V(a_1, a_2) \sim v^4 e^{-\frac{4}{b_{\text{QCD}}} \frac{8\pi^2}{g_{\text{QCD}}^2(v)}} \cos\left(\sum_i \frac{a_i}{f_i}\right) + v^4 \sum_i e^{-\frac{8\pi^2}{g_i^2(v)}} \cos\left(\frac{a_i}{f_i}\right). \quad (2.15)$$

Here, b_{QCD} is the coefficient of the one-loop β -function of the QCD gauge coupling.

Notably, the additional contributions from the small instantons lead to an increase in the axion mass. For example, when $g_1 = g_2$, we find

$$g_1^2(v) = g_2^2(v) = 2g_{\text{QCD}}^2(v), \quad (2.16)$$

and hence, the additional contributions become comparable to the QCD contribution. If we extend the gauge group from $\text{SU}(3)_1 \times \text{SU}(3)_2$ to $[\text{SU}(3)]^{n_s}$ ($n_s \gg 1$), where $\text{SU}(3)_{\text{QCD}}$ appears as the diagonal subgroup of $[\text{SU}(3)]^{n_s}$, the gauge coupling constant at each sector can be as large as $g_i^2(v) \sim n_s g_{\text{QCD}}^2(v)$. In such cases, further enhancement of the axion mass is possible [42].

In this discussion, we have neglected the effects of SM quarks for simplicity. Around (constrained) instantons of both QCD and the broken part, SM quarks exhibit zero modes. Consequently, instanton effects are suppressed by Yukawa coupling constants of SM quarks. Despite this suppression, however, small instanton effects can still lead to the enhancement of the axion mass, especially in the cases where $n_s \gg 1$ [42, 44].

3 Model of Composite Accidental Axion

In this section, we review the composite axion model in Refs. [32, 33] and the simplest CAA model in Ref. [36]. A key difference of this model from the example in Sec. 2.2 is the presence of new fermions. As we will see in Secs. 4 and 5, chiral symmetries of the new fermions reduce the small constrained instanton effects on the axion mass.

3.1 Composite Axion Model

In the original composite axion model proposed in Refs. [32, 33], a new $\text{SU}(N)$ confining gauge interaction called axicolor is introduced. Hereafter, the confining scale is assumed to be much higher than the electroweak scale. This model has left-handed Weyl fermions charged under $\text{SU}(N)$ and $\text{SU}(3)_{\text{QCD}}$ as,

$$(\mathbf{N}, \mathbf{3})_1 \oplus (\overline{\mathbf{N}}, \overline{\mathbf{3}})_1 \oplus (\mathbf{N}, \mathbf{1})_{-3} \oplus (\overline{\mathbf{N}}, \mathbf{1})_{-3}. \quad (3.1)$$

Here, the subscripts indicate the charges under the $\text{U}(1)_{\text{PQ}}$ symmetry, which is imposed by hand. In the limit of vanishing QCD coupling, this model exhibits a chiral flavor symmetry of $\text{SU}(4)_L \times \text{SU}(4)_R \times \text{U}(1)_V$.³ Within this framework, $\text{SU}(3)_{\text{QCD}}$ is embedded in the vector-like subgroup, i.e.,

³The flavor symmetry of \mathbf{N} fermions is denoted by $\text{SU}(4)_L$ and that of $\overline{\mathbf{N}}$ by $\text{SU}(4)_R$.

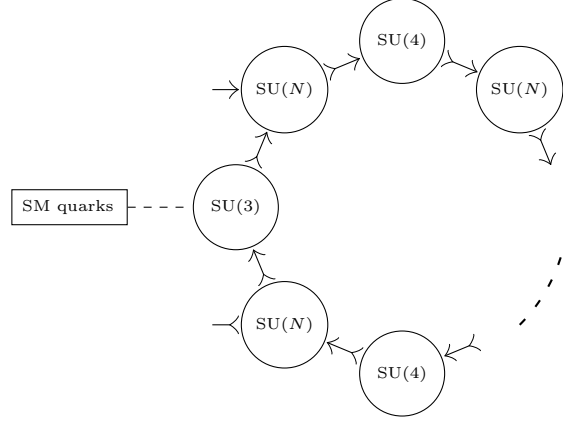


Figure 1: The moose diagram of the $SU(3) \times [SU(N)]^{n_s} \times [SU(4)]^{n_s-1}$ composite accidental axion model. The arrow \rightarrow denotes the fundamental representation fermion and the arrow \longleftarrow the anti-fundamental representation of the left-handed . We show tables of the model for $n_s = 2$ and 3 in Tabs. 1 and 2, respectively.

$SU(3)_{\text{QCD}} \subset SU(4)_V \subset SU(4)_L \times SU(4)_R$. The $U(1)_{\text{PQ}}$ symmetry is identified as an axial subgroup of $SU(4)_L \times SU(4)_R$, and is therefore anomaly-free with respect to $SU(N)$. Note that $U(1)_{\text{PQ}}$ is, on the other hand, anomalous with respect to $SU(3)_{\text{QCD}}$.

At the dynamical scale of $SU(N)$, Λ , the confinement occurs and the (approximate) chiral flavor symmetry is spontaneously broken, i.e., $SU(4)_L \times SU(4)_R \rightarrow SU(4)_V$, which includes the spontaneous breaking of $U(1)_{\text{PQ}}$. The corresponding 15 Goldstone modes including the axion are decomposed in terms of $SU(3)_{\text{QCD}}$ representations as,

$$\mathbf{15} = \mathbf{8} \oplus \mathbf{3} \oplus \bar{\mathbf{3}} \oplus \mathbf{1} . \quad (3.2)$$

The color singlet Goldstone boson corresponds to the QCD axion. The colored Goldstone modes obtain masses of $\mathcal{O}(g_{\text{QCD}}\Lambda)$ from the QCD radiative corrections. The key aspect of the composite axion model is the embedding of QCD and $U(1)_{\text{PQ}}$ into the $SU(4)_L \times SU(4)_R$ flavor symmetry in axicolor dynamics.

In the original composite axion model, the $U(1)_{\text{PQ}}$ symmetry is imposed by hand, and therefore, the model cannot address the axion quality problem. In the following section, we will discuss an extension of the composite axion model proposed in Ref. [36], where the $U(1)_{\text{PQ}}$ symmetry emerges accidentally.

3.2 $SU(3) \times SU(N)^{n_s} \times SU(4)^{n_s-1}$ Model

Gauge Group and Matter Content

In the composite accidental axion (CAA) model in Ref. [36], the axicolor is extended to a product group, $SU(N) \rightarrow [SU(N)]^{n_s}$ ($n_s \geq 2$). Each $SU(N)$ gauge sector (labeled as $SU(N)_{S_i}$ ($i = 1, \dots, n_s$)) consists of four pairs of fundamental and antifundamental left-handed Weyl fermions. The maximal flavor symmetry of each sector is $SU(4)_L \times SU(4)_R \times U(1)_V$ as in the case of the original composite axion model. The subgroups of the flavor symmetries are weakly gauged so that the model possess $[SU(N)]^{n_s} \times [SU(4)]^{n_s-1} \times SU(3)$ gauge symmetry. The moose diagram of the model is given in Fig. 1.

	SU(3) _w	SU(N) _{S1}	SU(4) _w	SU(N) _{S2}	U(1) _{PQ} ^(SSB)	U(1) ₁	U(1) _B	U(1) _B '
$\psi_{A_2}^c$	$\bar{\mathbf{3}}$	$\mathbf{1}$	$\mathbf{1}$	\mathbf{N}	1	1	1	1
ψ_{A_2}	$\mathbf{1}$	$\mathbf{1}$	$\mathbf{1}$	\mathbf{N}	-3	1	-3	1
$\psi_c^{A_1}$	$\mathbf{3}$	$\bar{\mathbf{N}}$	$\mathbf{1}$	$\mathbf{1}$	1	1	-1	-1
ψ^{A_1}	$\mathbf{1}$	$\bar{\mathbf{N}}$	$\mathbf{1}$	$\mathbf{1}$	-3	1	3	-1
$\psi_{A_1}^p$	$\mathbf{1}$	\mathbf{N}	$\bar{\mathbf{4}}$	$\mathbf{1}$	0	-1	0	1
$\psi_p^{A_2}$	$\mathbf{1}$	$\mathbf{1}$	$\mathbf{4}$	$\bar{\mathbf{N}}$	0	-1	0	-1

Table 1: The minimal model of the CAA with $n_s = 2$. The subscript ‘‘S’’ denotes the strong coupling while ‘‘w’’ denotes the weak coupling. The indices A_1 and A_2 of the left-handed Weyl fermions ψ 's are for the representations under $SU(N)_{S1}$ and $SU(N)_{S2}$. The indices c and p are for the representations under $SU(3)_w$ and $SU(4)_w$. The $U(1)_{PQ}$ symmetry is anomalous with respect to $SU(3)_w$, and the $U(1)_1$ symmetry is anomalous with respect to $SU(3)_w \times SU(4)_w$. The global $U(1)_B$ and $U(1)'_B$ symmetries are anomaly-free with respect to all the gauge groups. Blue and red columns highlight weakly and strongly coupled gauge interactions. The green columns highlight anomalous $U(1)$ symmetries with respect to weakly coupled gauge groups.

Each of n_s weakly gauged symmetries corresponds to the diagonal subgroup of the product of the $SU(4)_L$ flavor symmetry in the $SU(N)_{S_i}$ sector and the $SU(4)_R$ flavor symmetry in the $SU(N)_{S_{(i+1)}}$ sector, respectively. Among those n_s weakly coupled gauge symmetries, $n_s - 1$ of them are gauged as $SU(4)$ symmetries and the other one is gauged as $SU(3)$ symmetry. Altogether, the model has $[SU(N)]^{n_s} \times [SU(4)]^{n_s-1} \times SU(3)$ gauge symmetry. Due to the axicolor dynamics, the weakly gauged symmetry, $[SU(4)]^{n_s-1} \times SU(3)$, is spontaneously broken down to the diagonal subgroup which is identified with $SU(3)_{QCD}$. The QCD gauge coupling is given by the matching relation,

$$\frac{1}{g_{QCD}^2(\Lambda)} = \frac{1}{g_{3w}^2(\Lambda)} + \frac{1}{g_{4w,1}^2(\Lambda)} + \dots + \frac{1}{g_{4w,n_s-1}^2(\Lambda)}, \quad (3.3)$$

where $g_{3w}, g_{4w,1}, \dots$, and g_{4w,n_s-1} are gauge coupling constants with respect to $SU(3)_w, SU(4)_{w1}, \dots$, and $SU(4)_{w,n_s-1}$ respectively. Note that some of the gauge couplings on the right hand side can be significantly larger than g_{QCD} at the breaking scale Λ , which corresponds to the dynamical scale of the axicolor $SU(N)_{S_i}$ dynamics. For simplicity, we assume that the dynamical scales of Λ_i of $SU(N)_{S_i}$ are equal to Λ .

To illustrate how the model works, let us consider the simplest setup of the model with $n_s = 2$. The left-handed Weyl fermions in this example are listed in Tab. 1. In the table, ‘‘w’’ denotes the weak coupling. The gauge couplings of the two strong gauge symmetry are given by g_{S1}, g_{S2} , while those of weak $SU(3)_w$ and $SU(4)_w$ are given by g_3 and g_4 , respectively. Note that SM quarks are charged under $SU(3)_w$ gauge symmetry which are not shown in Tab. 1.

In the limit of vanishing weak gauge couplings, $g_3, g_4 \rightarrow 0$, the global symmetry is enhanced to the maximal symmetry $SU(4)_L \times SU(4)_R \times U(1)_V$ in each $SU(N)$ gauge sector. Hereafter, we call them $SU(4)_{Li} \times SU(4)_{Ri} \times U(1)_{Vi}$ ($i = 1, 2$), respectively. For $g_3 \neq 0$ and $g_4 \neq 0$, the flavor symmetries are reduced to four $U(1)$ symmetries. Two of them are $U(1)_{V1}$ and $U(1)_{V2}$. In the Tab. 1, we rearranged $U(1)_{V1}$ and $U(1)_{V2}$ into $U(1)_1$ and $U(1)'_B$, where $U(1)_1$ is anomalous with

	SU(3) _w	SU(N) _{S1}	SU(4) _{w1}	SU(N) _{S2}	SU(4) _{w2}	SU(N) _{S3}	U(1) _{PQ} ^(SSB)	U(1) ₁	U(1) _B	U(1) _B '	U(1) ₂
$\psi_{A_3}^c$	$\bar{\mathbf{3}}$	$\mathbf{1}$	$\mathbf{1}$	$\mathbf{1}$	$\mathbf{1}$	\mathbf{N}	$\mathbf{1}$	$\mathbf{1}$	$\mathbf{1}$	$\mathbf{1}$	$\mathbf{0}$
ψ_{A_3}	$\mathbf{1}$	$\mathbf{1}$	$\mathbf{1}$	$\mathbf{1}$	$\mathbf{1}$	\mathbf{N}	-3	$\mathbf{1}$	-3	$\mathbf{1}$	$\mathbf{0}$
$\psi_c^{A_1}$	$\mathbf{3}$	$\bar{\mathbf{N}}$	$\mathbf{1}$	$\mathbf{1}$	$\mathbf{1}$	$\mathbf{1}$	$\mathbf{1}$	$\mathbf{1}$	-1	-1	$\mathbf{0}$
ψ^{A_1}	$\mathbf{1}$	$\bar{\mathbf{N}}$	$\mathbf{1}$	$\mathbf{1}$	$\mathbf{1}$	$\mathbf{1}$	-3	$\mathbf{1}$	$\mathbf{3}$	-1	$\mathbf{0}$
$\psi_{A_1}^{p_1}$	$\mathbf{1}$	\mathbf{N}	$\bar{\mathbf{4}}$	$\mathbf{1}$	$\mathbf{1}$	$\mathbf{1}$	$\mathbf{0}$	-1	$\mathbf{0}$	$\mathbf{1}$	$\mathbf{0}$
$\psi_{p_1}^{A_2}$	$\mathbf{1}$	$\mathbf{1}$	$\mathbf{4}$	$\bar{\mathbf{N}}$	$\mathbf{1}$	$\mathbf{1}$	$\mathbf{0}$	$\mathbf{0}$	$\mathbf{0}$	-1	-1
$\psi_{A_2}^{p_2}$	$\mathbf{1}$	$\mathbf{1}$	$\mathbf{1}$	\mathbf{N}	$\bar{\mathbf{4}}$	$\mathbf{1}$	$\mathbf{0}$	$\mathbf{0}$	$\mathbf{0}$	$\mathbf{1}$	$\mathbf{1}$
$\psi_{p_2}^{A_3}$	$\mathbf{1}$	$\mathbf{1}$	$\mathbf{1}$	$\mathbf{1}$	$\mathbf{4}$	$\bar{\mathbf{N}}$	$\mathbf{0}$	-1	$\mathbf{0}$	-1	$\mathbf{0}$

Table 2: The CAA model with $n_s = 3$. This model possesses an extra U(1) symmetry U(1)₂, in addition to those in the model with $n_s = 2$. Since U(1)₂ is anomalous only with respect to SU(4)_{w2} and not broken spontaneously, it can be used to cancel the θ -angle of SU(4)_{w2}. Meanings of the colors are the same with those in Tab. 1.

respect to SU(3)_w × SU(4)_w, while U(1)_B' is free from anomaly. The other two are the vector/axial combinations of U(1) symmetries in the SU(4)_{L2} × SU(4)_{R1} flavor symmetry which commute with SU(3)_w. The axial combination is anomalous with respect to SU(3)_w and is identified with U(1)_{PQ}. The vector combination U(1)_B is anomaly-free.

Note that all the U(1) symmetries are realized as accidental ones at the renormalizable level. Mass terms are also prohibited by the same reason.⁴ Let us also comment on the θ -angles of each gauge groups denoted by θ_{S1} , θ_{S2} , θ_{w3} and θ_{w4} . As for θ_{S1} and θ_{S2} , they can be set to zero by two global U(1) rotations which are anomalous with respect SU(N)_{S1} and SU(N)_{S2}. The angles θ_{w3} and θ_{w4} can be set to zero by using U(1)_{PQ} and U(1)₁ rotations. Therefore, the θ -angles in this model do not spoil the axion mechanism. These arguments can be easily extended for $n_s > 2$. For example we show the model contents for $n_s = 3$ in Tab. 2.

Chiral Flavor Symmetry Breaking and Composite Axion

The dynamics of the CAA model is as follows. We assume that the strong gauge interactions of SU(N)_{Si} ($i = 1, 2$) exhibit confinement and chiral condensations at dynamical scales Λ_i . The VEVs of fermion bilinears are assumed to be

$$\begin{aligned}
\langle \psi_{A_1}^p \psi_{\bar{p}}^{A_1} \rangle &\sim \Lambda_1^3 \delta_{\bar{p}}^p, \\
\langle \psi_{A_2}^{\bar{p}} \psi_p^{A_2} \rangle &\sim \Lambda_2^3 \delta_{\bar{p}}^p,
\end{aligned} \tag{3.4}$$

where SU(3)_w-colored $\psi_{A_2}^c$ and SU(3)_w-singlet ψ_{A_2} are grouped together as $\psi_{A_2}^{\bar{p}} = (\psi_{A_2}^c, \psi_{A_2})$ and $\psi_c^{A_1}, \psi^{A_1}$ are also grouped together as $\psi_{\bar{p}}^{A_1} = (\psi_c^{A_1}, \psi^{A_1})$. Hereafter, we take $\Lambda_1 = \Lambda_2 = \Lambda$ for simplicity. The condensations in Eq. (3.4) spontaneously break SU(3)_w × SU(4)_w into SU(3) which is identified with SU(3)_{QCD}. The condensations also break U(1)_{PQ} spontaneously, while the other U(1) symmetries in Tab. 1 are not broken spontaneously by the condensations.⁵

⁴We can also consider a more generic weakly coupled gauge group SU(3)_w × [SU(m)_w] ^{$n_s - 1$} . To forbid PQ-breaking mass terms of the fermions, we need $m \geq 4$.

⁵As for U(1)_B, a linear combination of U(1)_B and a subgroup of SU(4)_w generated by the diag(1, 1, 1, -3) remains unbroken.

As a result of chiral condensations, the axion associated with $U(1)_{\text{PQ}}$ breaking appears as a composite state,

$$\begin{aligned}\psi_{A_1}^p \psi_c^{A_1} &\sim \Lambda^3 \delta^p_c e^{i\frac{a}{F_a}} \quad , \quad \psi_{A_1}^p \psi^{A_1} \sim \Lambda^3 \delta^p_4 e^{-3i\frac{a}{F_a}} \quad , \\ \psi_{A_2}^c \psi_p^{A_2} &\sim \Lambda^3 \delta^c_p e^{i\frac{a}{F_a}} \quad , \quad \psi_{A_2} \psi_p^{A_2} \sim \Lambda^3 \delta^4_p e^{-3i\frac{a}{F_a}} \quad .\end{aligned}\tag{3.5}$$

The domain of the axion is given by $a/F_a \in [0, 2\pi)$ with F_a being the axion decay constant of $\mathcal{O}(\Lambda)$. The $U(1)_{\text{PQ}}$ symmetry is anomalous under QCD, and hence, a plays a role of the QCD axion.

Let us comment on the other Goldstone bosons associated with the chiral symmetry breaking, $SU(4)_{Li} \times SU(4)_{Ri} \rightarrow SU(4)_{Vi}$ ($i = 1, 2$). In the limit of $g_3, g_4 \rightarrow 0$, there are 2×15 goldstone modes. The 15 modes of them are absorbed by the Higgs mechanism associated with the spontaneous gauge symmetry breaking, $SU(3)_w \times SU(4)_w \rightarrow SU(3)_{\text{QCD}}$. The other 15 modes including the axion are massless at the tree-level. Except for the axion, they obtain masses due to the radiative corrections from $SU(3)_w \times SU(4)_w$ gauge interactions, as in the case of the original composite axion model (see Eq. (3.2)). As a result, all the composite states made by the axicolor dynamics obtain large masses of $\mathcal{O}(\Lambda)$, except for the axion.

Axion Quality Problem

The advantage of the CAA model is that the PQ symmetry appears as an accidental symmetry at the renormalizable level. This accidental symmetry is, however, explicitly broken by non-renormalizable interactions. For $n_s = 2$, the lowest-dimensional operators which violate the PQ symmetry are

$$\mathcal{L}_{\text{PQ}} \sim \frac{\kappa}{M_{\text{Pl}}^2} \psi_c^{A_1} \psi_{A_1}^p \psi_p^{A_2} \psi_{A_2}^c + \text{h.c.} \quad ,\tag{3.6}$$

where M_{Pl} denotes the reduced Planck scale and κ is a numerical coefficient. This should be compared with the original composite axion model, where the mass terms of the fermions, which are allowed by any gauge symmetry can break the PQ symmetry explicitly.

The above argument can be extended straightforwardly for $n_s \geq 3$, where the lowest dimensional PQ symmetry breaking operators are

$$\mathcal{L}_{\text{PQ}} \sim \frac{\kappa}{M_{\text{Pl}}^{3n_s-4}} \psi_c^{A_1} \psi_{A_1}^{p_1} \cdots \psi_{p_{n_s-1}}^{A_{n_s}} \psi_{A_{n_s}}^c + \text{h.c.} \quad .\tag{3.7}$$

These PQ breaking terms result in an additional axion potential

$$V_{\text{PQ}} \sim |\kappa| \frac{\Lambda^{3n_s}}{M_{\text{Pl}}^{3n_s-4}} e^{2ia/F_a + \arg(\kappa)} + \text{h.c.} \quad ,\tag{3.8}$$

where we have assumed that the dynamical scales of all the strong $SU(N)$ sectors are comparable and of $\mathcal{O}(\Lambda)$, for simplicity. As a result, the VEV of the axion is shifted from zero to

$$\left\langle \frac{a}{F_a} \right\rangle \sim |\kappa| \left(\frac{\Lambda}{M_{\text{Pl}}} \right)^{3n_s} \left(\frac{M_{\text{Pl}}}{\Lambda_{\text{QCD}}} \right)^4 \arg(\kappa)\tag{3.9}$$

where we have used a rough estimate of the low-energy QCD contribution, $V \sim \Lambda_{\text{QCD}}^4 \cos(2Na/F_a)$. The axion quality problem is solved for $n_s \geq 4$, where the shift of the QCD θ -angle is well below the current constraints for $\Lambda \sim 10^{10}$ GeV. There are other possible PQ breaking operators which consist of baryonic composite operators of $SU(N)$. Contributions from these operators are suppressed for sufficiently large N .

4 Small Instanton Effects vs Chiral Symmetry

The CAA model in the previous section involves multiple broken gauge symmetries, and hence, constrained instantons potentially enhance the axion mass as we have seen in Sec. 2.2. In the CAA model, however, there are new fermions. In general, chiral symmetries of the fermions coupling to the axion have significant impacts on the axion mass.

In this section, we discuss the effect of chiral symmetries of the new fermions on the axion mass by considering a perturbative example which has the same breaking pattern of the weakly coupled gauge symmetries as well as the same chiral symmetries with the CAA model. We will discuss the axion mass in the CAA model in Sec. 5.

4.1 Toy Example: $SU(3)_w \times SU(4)_w$ Model

In the CAA model, the spontaneous breaking of the product gauge group, $SU(3)_w \times [SU(4)_w]^{n_s-1}$ is caused by the strong dynamics. Here, instead, we consider a model with gauge group $SU(3)_w \times SU(4)_w$ which is broken by condensations of complex scalar fields

$$\Phi_p^p (\mathbf{3} \oplus \mathbf{1}, \bar{\mathbf{4}}) , \quad \bar{\Phi}_{\tilde{p}}^{\tilde{p}} (\bar{\mathbf{3}} \oplus \mathbf{1}, \mathbf{4}) , \quad (4.1)$$

with the $SU(3)_w \times SU(4)_w$ representations in the parentheses. Here, p denotes an index of the $SU(4)_w$ fundamental representation, and \tilde{p} runs the $SU(3)_w$ color ($\tilde{p} = c = 1, 2, 3$) and the $SU(3)_w$ singlet ($\tilde{p} = 4$). This model mimics the CAA model with $n_s = 2$, by assuming that the VEVs of the scalars are given by,

$$\langle \Phi_p^p \rangle = v \delta_p^p , \quad \langle \bar{\Phi}_{\tilde{p}}^{\tilde{p}} \rangle = v \delta_{\tilde{p}}^{\tilde{p}} . \quad (4.2)$$

These VEVs break $SU(3)_w \times SU(4)_w$ into the diagonal subgroup $SU(3)$ as in the case of the CAA model. The unbroken subgroup is identified with $SU(3)_{\text{QCD}}$.

In this toy model, we restrict the scalar potential and its coupling to the fermions as

$$V = -m^2 \Phi^\dagger \Phi + \lambda (\Phi^\dagger \Phi)^2 + \xi \det \Phi + (\Phi \rightarrow \bar{\Phi}) - \kappa |\Phi \bar{\Phi}|^2 , \quad (4.3)$$

$$\mathcal{L}_{\text{int}} = -y_\Phi \bar{\psi}_1 \Phi \psi_2 - y_{\bar{\Phi}} \bar{\psi}_2 \bar{\Phi} \psi_1 + \text{h.c.} , \quad (4.4)$$

where λ , ξ , κ_Φ and $y_{\Phi, \bar{\Phi}}$ are coupling constants, and the mass parameter is $m^2 = \mathcal{O}(v^2)$. We take all the parameters real positive valued. All the global $U(1)$ symmetries of the toy model are listed in Tab. 3, which are the same with those in the CAA model in Tab. 1. Note that, unlike the CAA model, these symmetries are imposed by hand in Eqs. (4.3) and (4.4).

As in the case of the CAA model, the $U(1)_{\text{PQ}}$ symmetry and the weakly coupled $SU(3)_w \times SU(4)_w$ symmetries are spontaneously broken by the VEVs in Eq. (4.2) simultaneously. The corresponding axion appears in the phases,

$$\begin{aligned} \Phi_c^p &= v \delta_c^p e^{-i \frac{a}{F_a}} , & \Phi_4^p &= v \delta_4^p e^{3i \frac{a}{F_a}} , \\ \bar{\Phi}_p^c &= v \delta_p^c e^{-i \frac{a}{F_a}} , & \bar{\Phi}_p^4 &= v \delta_p^4 e^{3i \frac{a}{F_a}} . \end{aligned} \quad (4.5)$$

The axion decay constant is $F_a = \mathcal{O}(v)$. As in the case of the CAA model, $U(1)$ symmetries remain unbroken except for $U(1)_{\text{PQ}}$.

	SU(3) _w	SU(4) _w	U(1) _{PQ} ^(SSB)	U(1) ₁	U(1) _B	U(1) _B '
Φ_p^p	$\mathbf{3} \oplus \mathbf{1}$	$\bar{\mathbf{4}}$	$(-1, 3)$	0	$(-1, 3)$	0
$\bar{\Phi}_{\bar{p}}$	$\bar{\mathbf{3}} \oplus \mathbf{1}$	$\mathbf{4}$	$(-1, 3)$	0	$(1, -3)$	0
$\bar{\psi}_1^{\bar{p}}$	$\bar{\mathbf{3}} \oplus \mathbf{1}$	$\mathbf{1}$	$(1, -3)$	1	$(1, -3)$	1
$\psi_{1\bar{p}}$	$\mathbf{3} \oplus \mathbf{1}$	$\mathbf{1}$	$(1, -3)$	1	$(-1, 3)$	-1
$\bar{\psi}_2^p$	$\mathbf{1}$	$\bar{\mathbf{4}}$	0	-1	0	1
ψ_{2p}	$\mathbf{1}$	$\mathbf{4}$	0	-1	0	-1

Table 3: The toy model which mimics the CAA model with $n_s = 2$, where the gauge symmetry is broken by the VEVs of the scalar fields, Φ and $\bar{\Phi}$. Meanings of colors are similar to those in the CAA model.

Note that there is no additional Goldstone mode other than the axion and the would-be Goldstone modes associated with the gauge symmetry breaking, $SU(3)_w \times SU(4)_w \rightarrow SU(3)_{\text{QCD}}$. Note also that all the fermions obtain masses of $\mathcal{O}(v)$ through the Yukawa interactions and the VEVs in Eq. (4.2). As a result, this toy example leaves only the axion as a light particle as in the CAA model.

In the following discussion, we will neglect the effects of SM quarks to the axion potential. As we will see later, those effects are irrelevant when comparing the QCD instanton contributions with those from the small instantons.

4.2 Suppression of Instanton Effects by Anomalous Symmetry

Let us examine the impact of anomalous chiral symmetries on the axion mass within the $SU(3)_w \times SU(4)_w$ toy model. The axion mass can be obtained from the vacuum amplitude with a constant axion background field a ,

$$W(a)|_{m,n} = \int \mathcal{D}\bar{\psi}_1^\dagger \mathcal{D}\bar{\psi}_1 \mathcal{D}\psi_1^\dagger \mathcal{D}\psi_1 \mathcal{D}\bar{\psi}_2^\dagger \mathcal{D}\bar{\psi}_2 \mathcal{D}\psi_2^\dagger \mathcal{D}\psi_2 e^{-S_E[\psi, a]} . \quad (4.6)$$

Here m and n represent the winding numbers of $SU(3)_w$ and $SU(4)_w$ gauge field backgrounds, respectively. See Appendix A for notations of fermions in Euclidean space. The axion dependence of $S_E[\psi, a]$ appears through

$$\begin{aligned} \mathcal{L}_{\text{int}} = & -y_\Phi v e^{-i\frac{a}{F_a}} \bar{\psi}_1 \psi_2 |_{\text{colored}} - y_\Phi v e^{3i\frac{a}{F_a}} \bar{\psi}_1 \psi_2 |_{\text{singlet}} \\ & -y_{\bar{\Phi}} v e^{-i\frac{a}{F_a}} \bar{\psi}_2 \psi_1 |_{\text{colored}} - y_{\bar{\Phi}} v e^{3i\frac{a}{F_a}} \bar{\psi}_2 \psi_1 |_{\text{singlet}} . \end{aligned} \quad (4.7)$$

In the broken phase, the $U(1)_{\text{PQ}}$ transformation is realized by the phase rotations of ψ_1 's,

$$\psi_{1c} \rightarrow \psi'_{1c} = e^{i\alpha_{\text{PQ}}} \psi_{1c} , \quad \psi_{14} \rightarrow \psi'_{14} = e^{-3i\alpha_{\text{PQ}}} \psi_{14} , \quad (4.8)$$

$$\bar{\psi}_1^c \rightarrow \bar{\psi}_1^{c'} = e^{i\alpha_{\text{PQ}}} \bar{\psi}_1^c , \quad \bar{\psi}_1^4 \rightarrow \bar{\psi}_1^{4'} = e^{-3i\alpha_{\text{PQ}}} \bar{\psi}_1^4 , \quad (4.9)$$

and a shift of the axion,

$$\frac{a}{F_a} \rightarrow \frac{a}{F_a} + \alpha_{\text{PQ}} , \quad (4.10)$$

which leaves $S_E[\psi, a]$ invariant. By using the $U(1)_{\text{PQ}}$ transformation, we find that the vacuum amplitude satisfies,

$$W(a + \alpha_{\text{PQ}} F_a)|_{m,n} = e^{2mi\alpha_{\text{PQ}}} W(a)|_{m,n} , \quad (4.11)$$

where the phase factor appears due to the anomaly of $U(1)_{\text{PQ}}$ with respect to $SU(3)_w$. This confirms that the non-vanishing axion potential requires $m \neq 0$.

However, this is not the end of the story. In this toy model, as well as in the CAA model, there exists another anomalous symmetry, $U(1)_1$, which does not undergo spontaneous breaking. The $U(1)_1$ transformation is realized as

$$\psi_{1\bar{p}} \rightarrow \psi'_{1\bar{p}} = e^{i\alpha} \psi_{1\bar{p}} , \quad \bar{\psi}_1^{\bar{p}} \rightarrow \bar{\psi}'_1^{\bar{p}} = e^{i\alpha} \bar{\psi}_1^{\bar{p}} , \quad (4.12)$$

$$\psi_{2p} \rightarrow \psi'_{2p} = e^{-i\alpha} \psi_{2p} , \quad \bar{\psi}_2^p \rightarrow \bar{\psi}'_2^p = e^{-i\alpha} \bar{\psi}_2^p , \quad (4.13)$$

while the axion is not shifted. Note that the present model possesses two θ -angles, θ_3 and θ_4 , corresponding to $SU(3)_w$ and $SU(4)_w$, respectively. The anomalous $U(1)_1$ symmetry eliminates $\theta_3 - \theta_4$, leaving only QCD θ -angle, $\theta_3 + \theta_4$.

By using the $U(1)_1$ transformation, we find that the vacuum amplitude satisfies,

$$W(a)|_{m,n} = e^{2i\alpha(m-n)} W(a)|_{m,n} . \quad (4.14)$$

The phase factors appear from the $U(1)_1$ anomalies with respect to $SU(3)_w \times SU(4)_w$. As a result, $W(a)|_{m,n} = 0$ for $m \neq n$. This means that small instanton configurations can contribute to the axion mass only when the winding numbers of $SU(3)_w$ and $SU(4)_w$ are identical. We find that $U(1)_1$ symmetry, which eliminates $\theta_3 - \theta_4$, also restricts the small instanton effects on the axion mass. As we will see later, the null contributions for $m \neq n$ can also be understood as the effect of fermion zero modes in the path integration (see Sec. 4.4). Notice that this argument does not contradict with the non-vanishing axion potential from the QCD instantons in this model, since the QCD instantons have the winding number satisfying $m = n$.

It is instructive to note that the above discussion also stems from an ambiguity of the $U(1)_{\text{PQ}}$ symmetry. For example, we may redefine the PQ charge assignment from that in Tab. 3 to

$$Q'_{U(1)_{\text{PQ}}} = Q_{U(1)_{\text{PQ}}} + x Q_{U(1)_1} , \quad (4.15)$$

with an arbitrary factor x . In this case, Eq. (4.11) becomes,

$$W(a + \alpha_{\text{PQ}} F_a)|_{m,n} = e^{2mi\alpha_{\text{PQ}} + 2x(m-n)i\alpha_{\text{PQ}}} W(a) , \quad (4.16)$$

which is free from the ambiguity and can be non-vanishing, only for $m = n$.

4.3 Fermion Zero Modes and 't Hooft Operator

As we have seen, small instantons can contribute to the axion mass only when the winding numbers of the $SU(3)_w$ and $SU(4)_w$ backgrounds coincide. In the following, we estimate the axion mass from small instantons satisfying this condition.

To determine the non-vanishing effects of the instanton background, we must take into account the fermion zero modes around the instantons. In general, the Dirac operator \not{D} has normalizable

zero modes in the instanton background. In the case of the constrained instanton in the broken phase, it is notable that massive fermions also have normalized zero modes when they obtain masses from the gauge symmetry breaking field Φ [51]. More closely, the kinetic operators of those massive fermions are given by,

$$i\mathcal{D} - y\Phi(x) , \quad (4.17)$$

which have zero modes around the constrained instanton in the broken phase (see Appendix B). In the present toy model, there are zero modes in the fermions ψ 's around the constrained instanton associated with $SU(3)_w \times SU(4)_w \rightarrow SU(3)_{\text{QCD}}$, even though they become massive in the vacuum.

't Hooft Operator

To account for the effects of the fermion zero modes, it is useful to introduce the 't Hooft operator [53, 54]. For example, let us consider an $SU(N_c)$ gauge theory with N_f pairs of left-handed Weyl fermions of the fundamental (ψ_L) and the antifundamental representations ($\bar{\psi}_R$). In the following, we omit the index of the flavor. Around an instanton, ψ_L^\dagger and $\bar{\psi}_R^\dagger$ have normalizable zero modes. The effects of the path-integration over fermion zero modes can be captured by the insertion of a local operator at the position of the instanton. Such operator is called as 't Hooft operator, $\det_{N_f}(\psi_L \bar{\psi}_R)$. That is, we approximate the instanton effects by,

$$\int \mathcal{D}\psi^\dagger \mathcal{D}\psi \exp \left[- \int d^4x \left(\bar{\psi}_R i\mathcal{D}_E^{\text{inst}} \bar{\psi}_R^\dagger + \psi_L^\dagger i\mathcal{D}_E^{\text{inst}} \psi_L \right) \right] \quad (4.18)$$

$$\rightarrow \int \mathcal{D}\psi^\dagger \mathcal{D}\psi \left[\det_{N_f}(\psi_L \bar{\psi}_R) \exp \left[- \int d^4x \left(\bar{\psi}_R i\mathcal{D}_E \bar{\psi}_R^\dagger + \psi_L^\dagger i\mathcal{D}_E \psi_L \right) \right] \right] , \quad (4.19)$$

where D_μ^{inst} and D_μ are the covariant derivatives with/without the instanton background (see Appendix A). The determinant is taken over the N_f flavors, and the gauge and spinor indices of the fermions are contracted appropriately as in Ref. [53, 54]. Similarly, the anti-instanton contribution is proportional to $\det_{N_f}(\psi_L^\dagger \bar{\psi}_R^\dagger)$.

The 't Hooft operators are accompanied by the instanton factor and by the integration over sizes, that is [44],

$$\mathcal{C} \int \frac{d\rho}{\rho^5} \rho^{3N_f} \left(\frac{8\pi^2}{g^2} \right)^{2N_c} e^{-S_E(\rho^{-1})} \det_{N_f}(\psi_L \bar{\psi}_R) , \quad S_E(\rho^{-1}) = \frac{8\pi^2}{g^2(\rho^{-1})} . \quad (4.20)$$

Here, g represents the gauge coupling constant of $SU(N_c)$, and we have taken the renormalization scale to be the inverse of the small instanton size, $\mu = \rho^{-1}$ [53]. The coefficient \mathcal{C} is a dimensionless constant which depends on N_c and N_f . The 't Hooft operator reproduces the anomaly of the chiral $U(1)$ symmetry in the presence of an $SU(N_c)$ instanton.

't Hooft Operator in $SU(3)_w \times SU(4)_w$ Toy Model

Let us go back to the $SU(3)_w \times SU(4)_w$ axion toy model. As we have already mentioned, fermions have zero modes around $SU(3)_w$ and $SU(4)_w$ constrained instantons. Let us first discuss fermion

zero modes more closely. The fermion kinetic terms in Euclidean space are,

$$\begin{pmatrix} \psi_1^\dagger & \bar{\psi}_2 & \psi_2^\dagger & \bar{\psi}_1 \end{pmatrix} \begin{pmatrix} -i\bar{\sigma}^\mu D_\mu^{(3)} & -y_{\bar{\Phi}}\bar{\Phi}^\dagger & & \\ & -y_{\bar{\Phi}}\bar{\Phi} & i\sigma^\mu D_\mu^{(4)} & \\ & & -i\bar{\sigma}^\mu D_\mu^{(4)} & -y_\Phi\Phi^\dagger \\ & & -y_\Phi\Phi & i\sigma^\mu D_\mu^{(3)} \end{pmatrix} \begin{pmatrix} \psi_1 \\ \bar{\psi}_2^\dagger \\ \psi_2 \\ \bar{\psi}_1^\dagger \end{pmatrix}, \quad (4.21)$$

where $D_\mu^{(3)}$ and $D_\mu^{(4)}$ denote the $SU(3)_w$ and $SU(4)_w$ covariant derivatives, respectively. In the following, we take $y_\Phi = y_{\bar{\Phi}} = y$, for simplicity.

Following the discussions in Ref. [51], of which the result is also summarized in Appendix B, we see how fermion zero modes emerge around small instantons. Around an $SU(3)_w$ constrained instanton with a size $\rho \ll v^{-1}$, fermions $\bar{\psi}_1^\dagger$ and ψ_1^\dagger have zero modes accompanied by small $\mathcal{O}(\rho y v)$ contributions of ψ_2 and $\bar{\psi}_2$, respectively. When the instanton is at the origin, one of the zero mode wave functions is roughly expressed as,

$$\left(\psi_1^{\dagger(0)}(x), \bar{\psi}_2^{(0)}(x) \right) \sim \left(\frac{\rho}{(x^2 + \rho^2)^{3/2}}, \frac{\rho y v}{x^2 + \rho^2} \right), \quad (4.22)$$

for $x, \rho \ll v^{-1}$, while they are decaying exponentially at $x \gtrsim v^{-1}$. Around an anti-instanton, on the other hand, fermions which have zero modes can be obtained by exchanging $(\psi_1, \psi_2, \bar{\psi}_1, \bar{\psi}_2)$ and $(\psi_1^\dagger, \psi_2^\dagger, \bar{\psi}_1^\dagger, \bar{\psi}_2^\dagger)$, in Eq. (4.22). For $SU(4)_w$ (anti-)instantons, zero modes are obtained by exchanging $1 \leftrightarrow 2$.

The model corresponds to the case with $N_f = 1$ for both $SU(3)_w$ and $SU(4)_w$ sectors. Thus, the corresponding 't Hooft operator for the zero modes around $SU(3)_w$ instanton is

$$\left(\psi_1 + \mathcal{O}(\rho y v) \bar{\psi}_2^\dagger \right) \left(\bar{\psi}_1 + \mathcal{O}(\rho y v) \psi_2^\dagger \right), \quad (4.23)$$

while the 't Hooft operator for $SU(4)_w$ instantons is

$$\left(\psi_2 + \mathcal{O}(\rho y v) \bar{\psi}_1^\dagger \right) \left(\bar{\psi}_2 + \mathcal{O}(\rho y v) \psi_1^\dagger \right). \quad (4.24)$$

The gauge and spinor indices are implicit, and the operators are accompanied by the integrations over collective coordinates in Eq. (4.20). Note that zero modes in Eq. (4.23) and in Eq. (4.24) have $+1$ and -1 charges of $U(1)_1$, respectively. Accordingly, these 't Hooft operators reproduce the anomalies of the $U(1)_{PQ}$ and $U(1)_1$ symmetries in the presence of the instantons. Note that the differences of the $U(1)_{PQ}$ charges, for example between ψ_1 and $\bar{\psi}_2^\dagger$ in Eq. (4.23), are compensated by those of Φ 's. Hereafter, we omit $\mathcal{O}(\rho y v)$ contributions in the operators in Eqs. (4.23) and (4.24).

In the following, we denote the winding numbers m of $SU(3)_w$ sector and n of $SU(4)_w$ sector together by (m, n) . The 't Hooft operators for $(-1, 0)$ and $(0, -1)$ instantons are obtained by exchanging ψ 's and ψ^\dagger 's in the operators in Eqs. (4.23) and (4.24).

4.4 Non-vanishing Small Instanton Effects in $SU(3)_w \times SU(4)_w$ model

As we have discussed in Sec. 4.2, the small instanton effects can induce the axion potential only when the winding numbers of $SU(3)_w$ and $SU(4)_w$ backgrounds coincide with each other. Notice that the

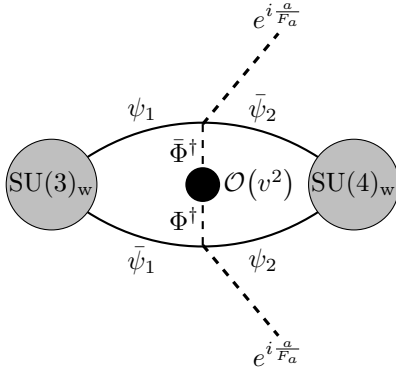


Figure 2: Non-vanishing contributions to the vacuum amplitude. Two gray blobs denote the 't Hooft vertices associated with an $SU(3)_w$ and an $SU(4)_w$ instanton, respectively. The axion dependence of the vacuum amplitude stems from the Yukawa interaction terms in Eq. (4.4). The black blob collectively describes the connection between Φ and $\bar{\Phi}$ through the couplings to the gauge bosons and the scalar potentials. In the figure, the effects of SM quarks are neglected.

null contributions from the $m \neq n$ configurations, as shown by Eq. (4.14) can also be understood through Feynman diagrammatic arguments using 't Hooft operators. In the presence of instanton configurations, the path integral vanishes unless all the fermion zero modes around the instantons are closed up diagrammatically. The numbers of the fermion zero modes $\psi_1, \bar{\psi}_1$ and $\psi_2, \bar{\psi}_2$ are equal to $2m$ and $2n$, respectively. Due to $U(1)_1$ symmetry, the difference between the numbers of fermion zero modes, $2m - 2n$, remains unchanged by interactions other than 't Hooft operators. Therefore, when $m \neq n$, some fermion zero modes cannot be closed up, causing the path integral to vanish.

The most relevant contributions are expected from $m = n = \pm 1$ backgrounds, and hence, let us first consider $(1, 0)$ and $(0, 1)$ instantons. In this case, non-vanishing vacuum amplitude appears through diagrams in Fig. 2 where two blobs denote the 't Hooft vertices associated with $SU(3)_w$ (i.e., $(1, 0)$) and $SU(4)_w$ (i.e., $(0, 1)$) instantons, respectively.

The contributions from $(1, 0)$ and $(0, 1)$ instantons are accompanied by the integrations over the sizes

$$\mathcal{O}_{(1,0)}(x_3) = \int \frac{d\rho_3}{\rho_3^5} \rho_3^3 e^{-\frac{8\pi^2}{g_3^2(\rho_3^{-1})}} \psi_1(x_3) \bar{\psi}_1(x_3), \quad \mathcal{O}_{(0,1)}(x_4) = \int \frac{d\rho_4}{\rho_4^5} \rho_4^3 e^{-\frac{8\pi^2}{g_4^2(\rho_4^{-1})}} \psi_2(x_4) \bar{\psi}_2(x_4), \quad (4.25)$$

respectively. The coordinates x_3 and x_4 are the positions of the instantons. Note that the integration of these operators over the position of the instanton is dimensionless. In the Feynman diagrams, the ultraviolet (UV) cutoff on the momentum which goes through a 't Hooft vertex is given by the inverse of its size, i.e. $\mathcal{O}(\rho^{-1})$. The infrared (IR) cutoff on the loop momentum is, on the other hand, given by v , below which the zero modes are exponentially damped. From the loop momentum integration, we find that the vacuum amplitude is roughly given by,

$$W(a)|_{m=n=1} \sim VT \times \int \frac{d\rho_3}{\rho_3^5} \frac{d\rho_4}{\rho_4^5} \rho_3^3 \rho_4^3 v^2 e^{-\frac{8\pi^2}{g_3^2(\rho_3^{-1})}} e^{-\frac{8\pi^2}{g_4^2(\rho_4^{-1})}} e^{2i\frac{a}{F_a}}, \quad (4.26)$$

where VT denotes the spacetime volume.

Now, let us consider the integrations over the instanton sizes $\rho_3, \rho_4 \lesssim v^{-1}$. To extract the size dependence of the classical actions, we rewrite the running couplings by using the one-loop coefficients of β -functions, b_3 and b_4 for $SU(3)_w$ and $SU(4)_w$,

$$\frac{8\pi^2}{g_i^2(\rho_i^{-1})} = \frac{8\pi^2}{g_i^2(v)} + b_i \log \frac{1}{\rho_i v}, \quad (i = 3, 4). \quad (4.27)$$

By substituting these expressions, the vacuum amplitude is given by

$$W(a)|_{m=n=1} \sim VT \times v^4 e^{-\frac{8\pi^2}{g_3^2(v)}} e^{-\frac{8\pi^2}{g_4^2(v)}} e^{2i\frac{a}{F_a}} \int^{v^{-1}} \frac{d\rho_3}{\rho_3} (\rho_3 v)^{b_3-1} \int^{v^{-1}} \frac{d\rho_4}{\rho_4} (\rho_4 v)^{b_4-1}. \quad (4.28)$$

These integrals are dominated by the contributions from instantons with sizes $\rho_3, \rho_4 \sim v^{-1}$ for $b_3, b_4 > 1$. As a result, the vacuum amplitude is reduced to,

$$W(a)|_{m=n=1} \sim VT \times v^4 e^{-\frac{8\pi^2}{g_{\text{QCD}}^2(v)}} e^{2i\frac{a}{F_a}}, \quad (4.29)$$

for $b_3, b_4 > 1$. Here, we have used the matching condition,

$$\frac{1}{g_{\text{QCD}}^2(v)} = \frac{1}{g_3^2(v)} + \frac{1}{g_4^2(v)}, \quad (4.30)$$

at the symmetry breaking scale.

By adding contributions from a pair of anti-instantons, we find that the amplitude in the small constrained instanton backgrounds for $m = n = \pm 1$ ends up with,

$$W(a)|_{m=n=1} + W(a)|_{m=n=-1} \sim VT \times v^4 e^{-\frac{8\pi^2}{g_{\text{QCD}}^2(v)}} \cos\left(\frac{2a}{F_a}\right). \quad (4.31)$$

Since $e^{-8\pi^2/g_{\text{QCD}}^2(v)}$ is small, we can use the dilute gas approximation, and we obtain the axion mass,

$$V(a)|_{\text{small instantons}} \sim v^4 e^{-\frac{8\pi^2}{g_{\text{QCD}}^2(v)}} \cos\left(\frac{2a}{F_a}\right), \quad (4.32)$$

for $b_3, b_4 > 1$. Similarly, for $m = n$ with $|n| \geq 2$, the instanton effects are proportional to $e^{-|n| \times 8\pi^2/g_{\text{QCD}}^2(v)}$. Consequently, these effects are much more suppressed compared to the contributions with $m = n = \pm 1$.

Note that in the present model, the small instanton effects cannot enhance the axion potential, even if one of the $SU(3)_w$ or $SU(4)_w$ couplings is significantly greater than the QCD coupling. This contrasts with the axion model without fermions discussed in Sec. 2.2. In that scenario, small instantons in each $SU(3)$ sector, such as the $(\pm 1, 0)$ and $(0, \pm 1)$ instantons, can independently contribute to the axion potential as described in Eq. (2.15). Consequently, the instanton effects can enhance the axion mass if one of the gauge couplings in the two sectors is much larger than the QCD coupling.

For the present model with fermions, small instantons with $m \neq n$ do not contribute to the axion potential because the fermion zero modes around the small instantons cannot be closed due to the chiral $U(1)_1$ symmetry in Tab. 3. To close up the fermion zero modes, non-vanishing contributions

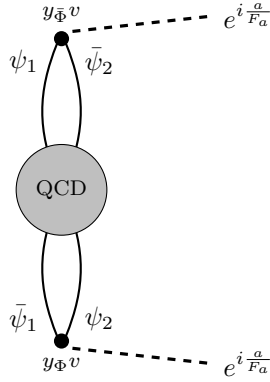


Figure 3: QCD instanton contribution to the vacuum amplitude with size of $\rho_{\text{QCD}} = \mathcal{O}(v^{-1})$. A gray blob denotes the 't Hooft vertex associated with QCD instanton. The axion dependence of the vacuum amplitude stems from the Yukawa interaction terms in Eq. (4.4) with Eq. (4.5). In the figure, the effects of SM quarks are neglected.

require $m = n$ small instantons in a connected diagram, as shown in Fig. 2. As a result, $n = m$ small instantons contribute collectively to the axion potential, and hence, the small instantons from the larger coupling sector are accompanied by weakly-coupled small instantons from the other sector. Due to the matching condition in Eq. (3.3), when one of the couplings is large, the other must be as small as the QCD coupling. Consequently, the collective instanton effects cannot enhance the axion potential.

Let us next consider the QCD (anti-)instanton effects of the similar instanton size, i.e., $\rho_{\text{QCD}} \sim v^{-1}$. Since QCD gauge group is realized as a diagonal subgroup of $\text{SU}(3)_w$ and $\text{SU}(4)_w$, QCD (anti-)instantons have the winding number (m, m) and automatically satisfy the non-vanishing condition of the vacuum amplitude in Eq. (4.14). Accordingly, for $\rho_{\text{QCD}} \sim v^{-1}$, the dominant contribution from the QCD (anti-)instanton is from $m = 1$, that is,

$$V(a)|_{\rho_{\text{QCD}} \sim v^{-1}} \sim v^4 e^{-\frac{8\pi^2}{g_{\text{QCD}}^2(v)}} \cos\left(\frac{2a}{F_a}\right). \quad (4.33)$$

A diagram for a QCD instanton contributing to the axion mass is shown in Fig. 3. The axion dependence appears from insertions of Eq. (4.5). This should be compared with Fig. 2, where we needed a scalar loop to obtain non-vanishing contributions. The difference stems from the fact that the ψ 's have the zero modes of the kinetic terms around the constrained instantons, while they do not around the the QCD instantons.

The above QCD instanton effects with a size of $\rho_{\text{QCD}} \sim v^{-1}$ can be also rewritten by using Λ_{QCD} ,

$$V(a)|_{\rho_{\text{QCD}} \sim v^{-1}} \sim \Lambda_{\text{QCD}}^4 \left(\frac{\Lambda_{\text{QCD}}}{v}\right)^{b_{\text{QCD}}-4} \cos\left(\frac{2a}{F_a}\right), \quad (4.34)$$

where $b_{\text{QCD}} = 7$ is the coefficient of the beta function of the QCD below the symmetry breaking scale v . Therefore, from Eqs. (4.32), (4.33) and (4.34), we find,

$$V_{\text{QCD}} \gg V(a)|_{\rho_{\text{QCD}} \sim v^{-1}} \sim V(a)|_{\text{small instantons}}, \quad (4.35)$$

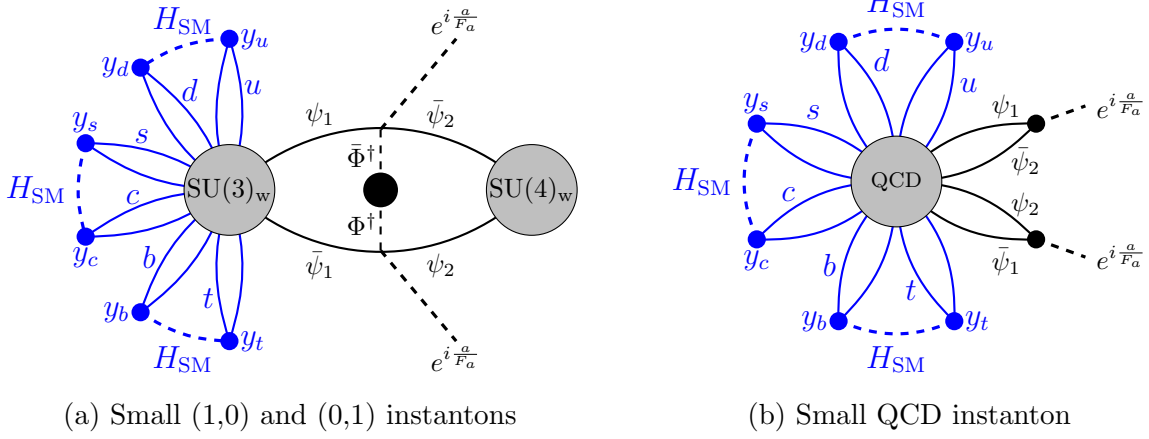


Figure 4: 't Hooft operators with SM quark zero modes closed by SM Higgs loops. In both figures, the instanton sizes are approximately $\rho \lesssim v^{-1}$, significantly smaller than the inverse electroweak scale. The SM contributions are highlighted in blue.

where $V_{\text{QCD}} \sim \Lambda_{\text{QCD}}^4 \cos(2a/F_a)$. Note that the second equality is valid for $b_3, b_4 > 1$. As a result, we find that the small instanton effects do not enhance the axion potential unlike in Sec. 2.2.

We have omitted the effects of SM quarks so far. Here, we will discuss the effects of the quark zero modes. Instanton effects become non-zero only when the quark zero modes are closed by mass insertions or some interactions. Since we are comparing the constrained instantons and small QCD instantons of sizes $\rho \sim v^{-1}$, the dominant contributions arise from closing the SM quark zero modes through SM Higgs loops, as illustrated in Fig. 4. These effects are common to both constrained instantons and QCD instantons of small scales, providing the suppression factor via SM quark Yukawa couplings,

$$D_y \simeq \prod_{i=u,d,s,c,b,t} \left(\frac{y_i}{4\pi} \right). \quad (4.36)$$

This factor is applied to the axion potential $V(a)|_{\rho_{\text{QCD}} \sim v^{-1}}$ and $V(a)|_{\text{small instantons}}$. Since this suppression is common to both QCD instanton contributions and constrained instanton contributions of similar sizes, the comparisons in Eq. (4.35) remain valid, even in the presence of SM quarks.

Two comments are in order. First, in Eq. (4.26), we have neglected the $\mathcal{O}(\rho_{3,4}^2 v^2)$ contributions in the classical action for the constrained instantons in Eq. (2.6). Since the integration over the instanton sizes is dominated by $\rho_3, \rho_4 \sim v^{-1}$, the $\mathcal{O}(\rho_{3,4}^2 v^2)$ contributions become sizable. In addition, we have also neglected the effect of overlapping of two constrained instantons. When two constrained instantons get close comparable to their respective sizes, i.e. $|x_3 - x_4| \lesssim \rho_{3,4}$, the configurations deviate from the isolated constrained instanton configurations. Thus, we expect that those effects enhance the value of the classical action, that is,

$$S_E > S_{E3}(v^{-1}) + S_{E4}(v^{-1}), \quad (4.37)$$

where $S_{E3,4}(\rho_{3,4})$ are the classical action for the isolated constrained instanton in Eq. (2.6). Since the vacuum amplitude is suppressed by e^{-S_E} , the larger S_E results in a smaller vacuum amplitude. Therefore, the small constrained instanton contributions estimated in this section should be regarded as rough upper limits.

Second, in the above discussion, we have assumed $b_3, b_4 > 1$. When $b_3, b_4 < 1$, on the other hand, the instantons with sizes much smaller than v^{-1} can be dominant and the estimate in Eq. (4.32) is altered. In the CAA model, we will see that the effects from instantons much smaller than the dynamical scale of the axicolor dynamics are more suppressed from a dynamical reason.

5 Small Instanton Effects on Composite Accidental Axion

Let us examine small instanton effects in the CAA model. Note that global symmetries and gauge groups relevant for the discussion of the axion mass are identical between the CAA model and the toy model in the previous section. In the following, we discuss the small instanton effects in the CAA model by repeating the arguments in the previous section.

5.1 Vanishing Small Instanton Effects

Let us consider the $n_s = 2$ model. We can extend the following discussion for $n_s > 2$ straightforwardly. As discussed in the previous section, the effects of SM quark zero modes can be incorporated with small instanton effects by applying the suppression factor in Eq. (4.36). In the following, we omit this factor, since it is irrelevant for the comparison between the effects of constrained instantons and small QCD instantons.

The axion mass can be again obtained from the vacuum amplitude with a constant axion background field a ,

$$W(a)|_{m,n} = \int \prod \mathcal{D}A_N \mathcal{D}\psi^\dagger \mathcal{D}\psi e^{-S_E[\psi, A_N]}, \quad (5.1)$$

where m and n represent the winding numbers of $SU(3)_w$ and $SU(4)_w$ gauge field backgrounds, respectively. Here, ψ and ψ^\dagger collectively denote the fermions, while A_N are the gauge fields of the axicolor $SU(N)_{S_i}$ dynamics. The axion dependence of Eq. (5.1) appears through Eqs. (3.5). Note again that the axicolor dynamics does not break the $U(1)_{PQ}$ symmetry, and hence, does not generate the axion potential by itself.

Now, let us consider the $U(1)_1$ rotation $\psi \rightarrow \psi'$ in Tab. 1,

$$\begin{aligned} \psi_{A_2}^{\tilde{p}} &= e^{i\alpha} \psi_{A_2}^{\tilde{p}}, & \psi_{\tilde{p}}^{\prime A_1} &= e^{i\alpha} \psi_{\tilde{p}}^{A_1}, \\ \psi_{A_1}^{\prime p} &= e^{-i\alpha} \psi_{A_1}^p, & \psi_p^{\prime A_2} &= e^{-i\alpha} \psi_p^{A_2}. \end{aligned} \quad (5.2)$$

Note that the axion is not affected by the $U(1)_1$ rotation. Under this rotation, the vacuum amplitude changes its phase as,

$$\begin{aligned} W(a)|_{m,n} &= \int \prod \mathcal{D}A_N \mathcal{D}\psi^{\prime\dagger} \mathcal{D}\psi' e^{-S_E[\psi', A_N]} \\ &= \int \prod \mathcal{D}A_N \mathcal{D}\psi^\dagger \mathcal{D}\psi \exp\left[2N \left(\int d^4x \frac{1}{32\pi^2} F_3^a F_3^{a\mu\nu} \tilde{F}_3^{a\mu\nu} - \int d^4x \frac{1}{32\pi^2} F_4^a F_4^{a\mu\nu} \tilde{F}_4^{a\mu\nu} \right) i\alpha \right] e^{-S_E[\psi, A_N]} \\ &= e^{2N(m-n)i\alpha} W(a)|_{m,n}. \end{aligned} \quad (5.4)$$

Here, F_3 and F_4 represent the field strengths of $SU(3)_w$ and $SU(4)_w$ gauge fields, respectively, and the second equality is the result of the chiral anomaly of $U(1)_1$. Therefore, as in the toy model, we find that the vacuum amplitude vanishes unless $m = n$.

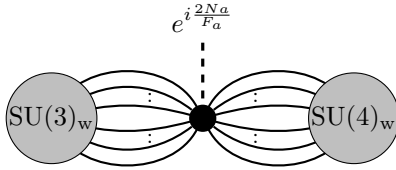


Figure 5: Non-vanishing contributions to the vacuum amplitude. Two gray blobs denote the 't Hooft vertices associated with an $SU(3)_w$ and an $SU(4)_w$ instanton, respectively. The black blob describes the effective interaction term in Eq. (5.6). As in Fig. 4a, there are SM quark zero modes around $SU(3)_w$ instanton, which are closed by SM Higgs loops. These are omitted in this figure.

5.2 Non-vanishing Small Instanton Effects

Let us consider the small instanton effects with $m = n$. In particular, we focus on the effects from a pair of $(\pm 1, 0)$ and $(0, \pm 1)$ instantons, which provide the dominant contribution to the axion potential.

Let us consider small constrained instantons with sizes $\rho \ll \Lambda^{-1}$, around which the fermions have zero modes of the kinetic terms. The relevant 't Hooft operators which encapsulate the effects of the zero modes around the $(1, 0)$ and $(0, 1)$ instantons in the CAA model are proportional to,

$$\mathcal{O}_{(1,0)} = \int \frac{d\rho_3}{\rho_3^5} \rho_3^{3N} e^{-\frac{8\pi^2}{g_3^2(\rho_3^{-1})}} \det_{A_1, A_2} (\psi_{A_2}^c \psi_{A_1}^{A_1}), \quad \mathcal{O}_{(0,1)} = \int \frac{d\rho_4}{\rho_4^5} \rho_4^{3N} e^{-\frac{8\pi^2}{g_4^2(\rho_4^{-1})}} \det_{A_1, A_2} (\psi_{A_1}^{p'} \psi_p^{A_2}), \quad (5.5)$$

where $\rho_3, \rho_4 \ll \Lambda^{-1}$ (see Eq. (4.20)). The integration of these operators over the position of the instanton is dimensionless. The determinants are taken over the axicolor indices.

In the toy model in the previous section, the 't Hooft operators $\mathcal{O}_{(1,0)}$ and $\mathcal{O}_{(0,1)}$ are connected through the Yukawa interactions with a scalar loop (see Fig. 2). In the CAA model, on the other hand, the operators $\mathcal{O}_{(1,0)}$ and $\mathcal{O}_{(0,1)}$ are connected through the effective interactions such as,

$$\mathcal{O}_{\text{sym}} \sim M^{4-6N} [(\psi_c^{A_1} \psi_{A_1}^p)(\psi_{A_2}^c \psi_p^{A_2})]^N \det_{A_1, A_2} (\psi_c^{\dagger A_2} \psi_{A_1}^{\dagger c}) \det_{A_1, A_2} (\psi_p^{\dagger A_1} \psi_{A_2}^{\dagger p}) + \text{h.c.}, \quad (5.6)$$

which are generated by the axicolor strong dynamics. Here, M denotes the Wilsonian cutoff scale for the effective operator. Let us emphasize that the operators generated by the axicolor dynamics do not violate the $U(1)_{PQ}$ and $U(1)_1$ symmetries, since those $U(1)$ symmetries are anomaly-free with respect to $SU(N)_{Si}$.

With the operator \mathcal{O}_{sym} , the fermion zero modes in $\mathcal{O}_{(1,0)}$ and $\mathcal{O}_{(0,1)}$ are closed up as shown in Fig. 5. The axion dependence appears by inserting Eqs. (3.5) to Eq. (5.6). To estimate the vacuum amplitude, let us assume that the integration over the loop momenta ℓ 's in Fig. 5 is dominated by $\ell \sim \ell_{\text{dom}}$, where ℓ_{dom} is in between $\Lambda \lesssim \ell_{\text{dom}} \lesssim \rho_{3,4}^{-1}$. In this case, we can crudely estimate the vacuum amplitude by substituting

$$M^{4-6N} \sim \ell_{\text{dom}}^{4-6N}, \quad (5.7)$$

$$[(\psi_c^{A_1} \psi_{A_1}^p)(\psi_{A_2}^c \psi_p^{A_2})]^N \sim \Lambda^{6N} e^{2Ni \frac{a}{F_a}}, \quad (5.8)$$

which results in

$$W(a)|_{m=n=1} \sim VT \times \int^{\Lambda^{-1}} \frac{d\rho_3}{\rho_3^5} \rho_3^{3N} e^{-\frac{8\pi^2}{g_3^2(\rho_3^{-1})}} \int^{\Lambda^{-1}} \frac{d\rho_4}{\rho_4^5} \rho_4^{3N} e^{-\frac{8\pi^2}{g_4^2(\rho_4^{-1})}} \times \ell_{\text{dom}}^{-4} \times \Lambda^{6N} e^{2Ni \frac{a}{F_a}}. \quad (5.9)$$

By noting $\ell_{\text{dom}}^{-1} \lesssim \Lambda^{-1}$, we find that the size of the vacuum amplitude from the small instanton contributions is limited as,

$$\begin{aligned} \left| W(a)|_{m=n=1} \right| &\lesssim VT \times \int^{\Lambda^{-1}} \frac{d\rho_3}{\rho_3^5} \rho_3^{3N} e^{-\frac{8\pi^2}{g_3^2(\rho_3^{-1})}} \int^{\Lambda^{-1}} \frac{d\rho_4}{\rho_4^5} \rho_4^{3N} e^{-\frac{8\pi^2}{g_4^2(\rho_4^{-1})}} \times \Lambda^{6N-4} \\ &\sim VT \times \Lambda^4 e^{-\frac{8\pi^2}{g_3^2(\Lambda)}} e^{-\frac{8\pi^2}{g_4^2(\Lambda)}} \int^{\Lambda^{-1}} \frac{d\rho_3}{\rho_3} (\rho_3 \Lambda)^{b_3+3N-4} \int^{\Lambda^{-1}} \frac{d\rho_4}{\rho_4} (\rho_4 \Lambda)^{b_4+3N-4}. \end{aligned} \quad (5.10)$$

Here, we have used the running gauge coupling constants in Eq. (4.27) to obtain the final expression. The IR cutoff of the integration over $\rho_{3,4}$ is of $\mathcal{O}(\Lambda^{-1})$.

From this expression, we find that the integration over the instanton sizes is dominated by the IR contribution, i.e., $\rho_{3,4} \simeq \Lambda^{-1}$, for

$$b_{3,4} > 4 - 3N. \quad (5.11)$$

As the β -function coefficients in the CAA model are given by,

$$b_3 = b_{\text{QCD}} - \frac{2}{3}N = 7 - \frac{2}{3}N, \quad (5.12)$$

$$b_4 = \frac{44}{3} - \frac{2}{3}N, \quad (5.13)$$

the condition (5.11) is satisfied for both $\text{SU}(3)_w$ and $\text{SU}(4)_w$ with $N > 0$. Therefore, in the CAA model, the crude upper limit on the vacuum amplitude from the small constrained instanton effects is given by,

$$\left| W(a)|_{m=n=1} \right| \lesssim VT \times \Lambda^4 e^{-\frac{8\pi^2}{g_3^2(\Lambda)}} e^{-\frac{8\pi^2}{g_4^2(\Lambda)}}. \quad (5.14)$$

Accordingly, the axion potential from the small instanton effects is at most,

$$V(a)|_{\text{small instantons}} \sim \Lambda^4 e^{-\frac{8\pi^2}{g_{\text{QCD}}^2(\Lambda)}} \cos\left(\frac{2Na}{F_a}\right). \quad (5.15)$$

Here, we have used the matching condition in Eq. (4.30) at Λ . In the presence of SM quarks, the suppression factor in Eq. (4.36) is applied to the above contribution. This factor is common to both constrained instantons and small QCD instantons.

We have found that the small instanton effects do not enhance the axion mass in the CAA model. This observation is similar to the case of the toy model discussed in Sec. 4.4. Specifically, small instantons with $m \neq n$ do not contribute to the axion potential due to the chiral $\text{U}(1)_1$ symmetry shown in Tab. 1. The collective $m = n$ instanton effects are suppressed by $e^{-|m| \times 8\pi^2 / g_3^2(\Lambda)} \times e^{-|n| \times 8\pi^2 / g_4^2(\Lambda)}$, which coincides with $e^{-|n| \times 8\pi^2 / g_{\text{QCD}}^2(\Lambda)}$ due to the matching condition of the QCD coupling in Eq. (3.3).

Several comments are in order. First, in Eq. (5.9), we have used Eq. (5.8) regardless of the size of the dominant loop momentum ℓ_{dom} . This substitution overestimates the size of the vacuum amplitudes if $\ell_{\text{dom}} \gg \Lambda$, since the condensation of the fermion bilinears disappear at the scale much higher than Λ . Second, we have also neglected the $\mathcal{O}(\rho^2 \Lambda^2)$ contributions to the classical action for the constrained instantons. Third, we have also neglected the increase of the value of the classical action due to the overlapping of the constrained instantons. These two effects lead to an underestimation of the classical action and therefore to an overestimation of the vacuum amplitude. Putting altogether, the small constrained instanton contributions estimated in this section should be regarded as rough upper limits.

5.3 Small Instanton Effects for $n_s > 2$

Finally, we mention the CAA models with $n_s > 2$. In the above discussion for $n_s = 2$, the $U(1)_1$ global symmetry plays an important role to show that only the $m = n$ instantons contribute to the axion potential. The crucial feature of $U(1)_1$ is that it is free from the axicolor anomaly and also not broken spontaneously by the axicolor dynamics, while being anomalous with respect to $SU(3)_w \times SU(4)_w$. In models with $n_s > 2$, we have $n_s - 1$ global $U(1)$ symmetries, $U(1)_i$ ($i = 1, \dots, n_s - 1$), which have the same roles of $U(1)_1$ in the model with $n_s = 2$. For example, $n_s = 3$ model possesses $U(1)_2$ in Tab. 2, in addition to $U(1)_1$.

In the model with $n_s \geq 2$, the vacuum amplitudes are labeled by the winding numbers of $SU(3)_w$, $SU(4)_{w,1}, \dots, SU(4)_{w,n_s-1}$ sectors denoted by $(m, n_1, \dots, n_{n_s-1})$. Under the $n_s - 1$ anomalous $U(1)$ transformations, the vacuum amplitude labeled by $(m, n_1, \dots, n_{n_s-1})$ changes its phase as

$$W(a)|_{m,n_1,\dots,n_{n_s-1}} = e^{i\alpha_1(2m-n_1-n_{n_s-1})} e^{i\alpha_2(n_2-n_1)} \dots e^{i\alpha_{n_s-1}(n_{n_s-1}-n_{n_s-2})} \times W(a)|_{m,n_1,\dots,n_{n_s-1}}, \quad (5.16)$$

where α_i ($i = 1, \dots, n_s - 1$) are the rotation angles of $U(1)_i$ transformations. Thus, we again find that the contributions from the small constrained instantons vanish unless

$$m = n_1 = \dots = n_{n_s-1}. \quad (5.17)$$

As a result, by repeating the discussion in Sec. 5.2, we find that the small instanton effects are at most

$$V(a)|_{\text{small instanton}} \sim \Lambda^4 e^{-\frac{8\pi^2}{g_{\text{QCD}}^2(\Lambda)}} \cos\left(\frac{2Na}{F_a}\right). \quad (5.18)$$

Here, the QCD coupling is matched to the gauge couplings of $SU(3)_w \times [SU(4)_w]^{n_s-1}$ via

$$\frac{1}{g_{\text{QCD}}^2(\Lambda)} = \frac{1}{g_{3w}^2(\Lambda)} + \frac{1}{g_{4w,1}^2(\Lambda)} + \dots + \frac{1}{g_{4w,n_s-1}^2(\Lambda)}, \quad (5.19)$$

at the symmetry breaking scale Λ . Therefore, the axion mass is not enhanced by small constrained instantons, also in the case of $n_s > 2$.

6 Application to Other Composite Axion Models

As we have learned in the previous section, the small instanton effects do not enhance the axion mass in the CAA model. In this section, let us extend our discussion to other types of composite axion models.

6.1 Composite Axion Models with Spectator QCD

Let us first consider a class of composite axion models in which $SU(3)_{\text{QCD}}$ does not take part in the chiral symmetry breaking caused by the axicolor dynamics. Specifically, we examine a model with gauge symmetry of $G_S \times G_w \times SU(3)_{\text{QCD}}$ where G_S represents the axicolor gauge group, and G_w is a weakly gauged subgroup of flavor symmetry. In these models, the axicolor dynamics only

spontaneously breaks G_w . QCD, therefore, acts as a spectator to the axicolor dynamics. The original composite axion model in Ref. [33] (see Sec. 3.1) is one of the examples.

In this class of models, extensions have been proposed to solve the axion quality problem by adding a new chiral gauge symmetry to the original composite axion model [34, 41], by replacing axicolor dynamics with chiral axicolor dynamics [39], or by incorporating supersymmetry [38]. Note that $SU(3)_{\text{QCD}}$ does not mix with the other gauge groups when PQ breaking occurs. By construction, the PQ symmetry is only anomalous with respect to QCD. Therefore, in this class of models, there are no additional instanton effects on the axion potential other than those from QCD. This conclusion is different from the case in the CAA model discussed in the previous section, where the constrained instantons have small but non-vanishing contributions to the axion mass.

6.2 Axial $SU(3) \times [SU(N)]^{n'_s} \times [SU(m)]^{n'_s}$ Model

In Sec. 3.2, we discussed the CAA model, which features $SU(3) \times [SU(N)]^{n_s} \times [SU(4)]^{n_s-1}$ gauge groups. In this model, the $SU(3)$ and $SU(4)$ groups are embedded in the vector-like subgroups of the $SU(4)_L \times SU(4)_R$ flavor symmetry, associated with each axicolor $SU(N)$ gauge dynamics. In contrast, Ref. [36] also proposes another model with $SU(3) \times [SU(N)]^{n'_s} \times [SU(m)]^{n'_s}$ gauge groups, where $SU(m)$ and $SU(3)$ are embedded in the axial part of the flavor symmetries of the axicolor $[SU(N)]^{n'_s}$.

For $n'_s = 1$, for example, the model includes left-handed Weyl fermions with the following gauge charges:

$$(\mathbf{N}, \mathbf{m}, \mathbf{1}) \oplus (\mathbf{N}, \bar{\mathbf{m}}, \mathbf{1}) \oplus (\bar{\mathbf{N}}, \mathbf{1}, \mathbf{3}) \oplus (\bar{\mathbf{N}}, \mathbf{1}, \bar{\mathbf{3}}) \oplus (\bar{\mathbf{N}}, \mathbf{1}, \mathbf{1}) \times 2(m-3), \quad (6.1)$$

where the first, second, and third entries in the parentheses denote the representations under the $SU(N)$, $SU(m)$, and $SU(3)$ gauge groups, respectively. The fundamental and anti-fundamental fermions of $SU(N)$ exhibit $SU(2m)_L$ and $SU(2m)_R$ flavor symmetries, respectively. The $2m$ fundamental fermions are decomposed into $\mathbf{m} \oplus \bar{\mathbf{m}}$ representations of $SU(m) \subset SU(2m)_L$, while the $2m$ anti-fundamental fermions are decomposed into $\mathbf{3} \oplus \bar{\mathbf{3}} \oplus (\mathbf{1} \times 2(m-3))$ representations of $SU(3) \subset SU(2m)_R$.

This model can be derived by deforming the $SU(3) \times [SU(N)]^{n_s} \times [SU(4)]^{n_s-1}$ model in Sec. 3.2, with $n_s = 2n'_s$. Specifically, we pair i -th $SU(N)$ with $(n_s - i + 1)$ -th $SU(N)$ ($i = 1 \cdots n'_s$), and identify one of the $SU(N)$ symmetries with the complex conjugate of the other. In Fig. 6, we illustrate this deformation with moose diagrams of the $SU(3) \times [SU(N)]^{n_s} \times [SU(4)]^{n_s-1}$ model and the axial $SU(3) \times [SU(N)]^{n'_s} \times [SU(4)]^{n'_s}$ model, specifically for $n_s = 2$.

In this model, the low energy QCD emerges as the diagonal subgroup of $SU(m)$'s and $SU(3)$ as in the case of the model in Sec. 3.2. The composite axion appears as one of the Goldstone modes, resulting from the spontaneous breaking of the generators of $SU(2m)_R$ which commute with $SU(3)_{\text{QCD}}$.

Since $SU(3)_{\text{QCD}}$ appears as the diagonal subgroup of $SU(m) \times SU(3)$, constrained instantons can contribute to the axion potential. Similar to the CAA model in Sec. 3.2, we find that the model possesses $U(1)$ symmetries that are free from the axicolor anomaly but are anomalous with respect to $SU(m)$ and $SU(3)$. For example, consider the $U(1)$ symmetry with the charge assignment indicated by the subscripts:

$$(\mathbf{N}, \mathbf{m}, \mathbf{1})_{-1} \oplus (\mathbf{N}, \bar{\mathbf{m}}, \mathbf{1})_{-1} \oplus (\bar{\mathbf{N}}, \mathbf{1}, \mathbf{3})_1 \oplus (\bar{\mathbf{N}}, \mathbf{1}, \bar{\mathbf{3}})_1 \oplus (\bar{\mathbf{N}}, \mathbf{1}, \mathbf{1})_1 \times 2(m-3). \quad (6.2)$$

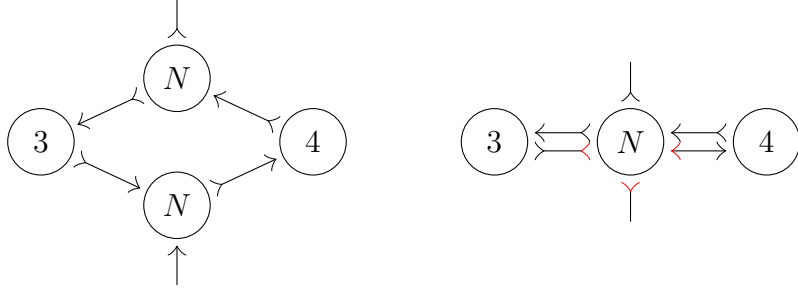


Figure 6: The moose diagrams for the $SU(3) \times [SU(N)]^{n_s} \times [SU(4)]^{n_s-1}$ model in Sec. 3.2 (see Tab. 1), and for the axial $SU(3) \times [SU(N)]^{n'_s} \times [SU(4)]^{n'_s}$ model when $n_s = 2$ and $m = 4$. An arrow \rightarrow represents the fundamental representation, and an arrow \succleftarrow represents the antifundamental representation. From the $SU(3) \times [SU(N)]^2 \times SU(4)$ model, the axial $SU(3) \times SU(N) \times SU(4)$ model is derived by identifying the upper $SU(N)$ with the complex conjugate of the lower $SU(N)$, which is indicated by flipping the arrow heads colored in red. Extending these models to cases with $n'_s > 1$ is straightforward.

This $U(1)$ symmetry remains unbroken and is anomalous with respect to $SU(m)$ and $SU(3)$. Note that this anomalous but unbroken $U(1)$ symmetry corresponds exactly to $U(1)_1$ as discussed in Tab. 1 in the previous section.

By revisiting the discussion in Sec. 5.1, which is based on $U(1)_1$, we find that small constrained instantons affect the axion potential only when the winding numbers of $SU(m)$'s and $SU(3)$ are identical. Furthermore, the arguments in Sec. 5.2 using 't Hooft operators demonstrate that constrained instantons which are significantly smaller than the inverse of the dynamical scale are irrelevant for the axion potential. Consequently, we again find that the small instanton effects contribute to the axion potential at most as follows:

$$V(a)|_{\text{small instanton}} \sim \Lambda^4 e^{-\frac{8\pi^2}{g_{\text{QCD}}^2(\Lambda)}} \cos\left(\frac{2Na}{F_a}\right), \quad (6.3)$$

which is subdominant compared with the axion potential generated by low-energy QCD.

7 Conclusions

In this paper, we have discussed the small instanton effects in the composite accidental axion (CAA) models proposed in Ref. [36], where the $U(1)_{\text{PQ}}$ symmetry emerges as an accidental global symmetry. In these models, $SU(3)_{\text{QCD}}$ emerges as an unbroken diagonal subgroup of the product gauge group along with the spontaneous breaking of PQ symmetry by axicolor dynamics. The models feature instanton configurations which do not appear in the low-energy QCD, with sizes smaller than the inverse of the PQ symmetry breaking scale $f_a \sim \Lambda$. In some axion models, these configurations can significantly enhance the axion mass compared with the QCD effects. Indeed, the axion masses can be significantly enhanced by small instanton effects in models where the axions directly couple to the product gauge groups from which QCD appears as the unbroken subgroup [42], as we have seen in Sec. 2.2.

In the CAA models, there exist small instanton configurations in each SU(3) and SU(4) gauge group which do not appear in QCD. We have confirmed that small instantons in the broken part of the product group do contribute to the axion mass independently of those in QCD. However, we have also found that these contributions to the axion mass are negligibly small compared to the QCD contributions. As a result, the axion mass is not enhanced by the small instanton effects in the CAA models.

The crucial feature of the CAA models is that the models possess global chiral U(1) symmetries which are not broken spontaneously but are anomalous with respect to the weakly coupled gauge groups, such as $SU(3)_w \times [SU(4)_w]^{n_s-1}$. These U(1) symmetries, which correspond to $U(1)_1$ in Tab. 1 for the $n_s = 2$ model and to $U(1)_1 \times U(1)_2$ in Tab. 2 for the $n_s = 3$ model, play a crucial role in solving the strong CP problem by eliminating θ -terms in the hidden sectors. In generic n_s -site models, there are $n_s - 1$ such U(1) symmetries. In generic n_s -site models, there are $n_s - 1$ such U(1) symmetries.

In this work, we have shown that these U(1) symmetries are also essential in suppressing the small instanton effects. In the CAA models, small instantons do not contribute to the axion potential unless winding numbers of all the SU(3) and SU(4) sectors are identical. This occurs because the fermion zero modes around the small instantons cannot be closed due to those chiral U(1) symmetries. In the $n_s = 2$ model for example, non-vanishing contributions require multiple small instantons in a connected diagram to close up the fermion zero modes, as shown in Fig. 5. As a result, small instantons with identical winding number for all the unconfined sectors contribute collectively to the axion potential. Thus, the small instantons from the larger coupling sector are accompanied by weakly-coupled small instantons from other sectors. Consequently, the small instanton effects do not enhance the axion mass, as they are suppressed by a collective instanton factor, $e^{-|m| \times 8\pi^2 / g_{3w}^2} \times e^{-|n_1| \times 8\pi^2 / g_{4w,1}^2} \times \dots \times e^{-|n_{n_s-1}| \times 8\pi^2 / g_{4w,n_s-1}^2}$. With the same winding numbers from all the sectors, $m = n_1 = \dots = n_{n_s-1}$, this coincides with $e^{-|m| \times 8\pi^2 / g_{\text{QCD}}^2}$ due to the matching condition of the QCD coupling in Eq. (3.3). These small instanton effects are dominated by those with sizes around the inverse of the PQ breaking scale, Λ^{-1} . As a result, we find that small constrained instanton effects on the axion mass are at most comparable to the effects of QCD instantons of the same size, $\rho_{\text{QCD}} \sim \Lambda^{-1}$. Therefore, they are negligible compared with the low-energy QCD effects.

In conclusion, we emphasize that the presence of anomalous U(1) symmetries, which are not spontaneously broken, significantly restricts the impact of small instanton effects on the axion potential. This finding is crucial for understanding the influence of small instantons on the axion potential across a wide range of axion models with high-quality PQ symmetry, not just limited to the CAA models. It highlights the challenge of increasing the axion mass without spoiling the high-quality PQ symmetry.

Acknowledgements

TA acknowledges Sungwoo Hong and Ryosuke Sato for valuable communications. This work is supported by Grant-in-Aid for Scientific Research from the Ministry of Education, Culture, Sports, Science, and Technology (MEXT), Japan, 20H01895 and 20H05860 (S.S.), 21H04471 and 22K03615 (M.I.) and by World Premier International Research Center Initiative (WPI), MEXT, Japan. This work is supported by JST SPRING Grant Number JPMJSP2108 (K.W.). This work is also supported by FoPM, WINGS Program, the University of Tokyo (T.A.).

A Notation and Remarks on Euclidean Space

A.1 Notation in Euclidean Space

We adopt the following notation for coordinates and derivatives in Minkowski spacetime and Euclidean space related via

$$x_{\text{E}}^i = x^i, \quad \partial_{\text{E}}^i = \partial_i, \quad x_{\text{E}}^4 = ix^0, \quad \partial_{\text{E}}^4 = -i\partial_0, \quad (\text{A.1})$$

for $i = 1, 2, 3$. The metric tensors are defined by,

$$g_{\mu\nu} = (+1, -1, -1, -1), \quad (\text{A.2})$$

in Minkowski spacetime and

$$g_{\mu\nu}^{\text{E}} = (+1, +1, +1, +1), \quad (\text{A.3})$$

in Euclidean space. The gauge potentials are also related via

$$A_{\text{E}}^i = A_i, \quad A_{\text{E}}^4 = -iA_0. \quad (\text{A.4})$$

In Minkowski spacetime, we use

$$(\sigma_{\text{M}}^{\mu})_{\alpha\dot{\alpha}} = (\mathbb{1}_2, \boldsymbol{\sigma}), \quad (\bar{\sigma}_{\text{M}}^{\mu})^{\dot{\alpha}\alpha} = (\mathbb{1}_2, -\boldsymbol{\sigma}), \quad (\mu = 0, 1, 2, 3), \quad (\text{A.5})$$

while we use

$$(\sigma_{\text{E}}^{\mu})_{\alpha\dot{\alpha}} = (\boldsymbol{\sigma}, i\mathbb{1}_2), \quad (\bar{\sigma}_{\text{E}}^{\mu})^{\dot{\alpha}\alpha} = (\boldsymbol{\sigma}, -i\mathbb{1}_2), \quad (\mu = 1, 2, 3, 4) \quad (\text{A.6})$$

in Euclidean space as in Ref. [51]. Here, $\boldsymbol{\sigma}$ denote Pauli matrices. The generators of the Lorentz group, $\bar{\sigma}_{\mu\nu}$, are defined by

$$\sigma_{\mu\nu} = \frac{1}{4i}(\bar{\sigma}_{\mu}\sigma_{\nu} - \bar{\sigma}_{\nu}\sigma_{\mu}), \quad \bar{\sigma}_{\mu\nu} = \frac{1}{4i}(\sigma_{\mu}\bar{\sigma}_{\nu} - \sigma_{\nu}\bar{\sigma}_{\mu}). \quad (\text{A.7})$$

We also define the corresponding generators in Euclidean space similarly from σ_{E}^{μ} and $\bar{\sigma}_{\text{E}}^{\mu}$.

For the generators of the SU(2) gauge group, we use the Pauli matrices $\boldsymbol{\tau}$. To describe the instanton solution, we use

$$(\tau^{\mu}) = (\boldsymbol{\tau}, \mathbb{1}_2), \quad (\bar{\tau}^{\mu}) = (\boldsymbol{\tau}, -i\mathbb{1}_2), \quad (\mu = 1, 2, 3, 4), \quad (\text{A.8})$$

and

$$\tau_{\mu\nu} = \frac{1}{4i}(\bar{\tau}_{\mu}\tau_{\nu} - \bar{\tau}_{\nu}\tau_{\mu}), \quad \bar{\tau}_{\mu\nu} = \frac{1}{4i}(\tau_{\mu}\bar{\tau}_{\nu} - \tau_{\nu}\bar{\tau}_{\mu}). \quad (\text{A.9})$$

Finally, we use the following notation for the two-dimensional anti-symmetric tensors,

$$\epsilon^{12} = -\epsilon^{21} = 1, \quad \epsilon_{12} = -\epsilon_{21} = -1, \quad \epsilon_1^2 = -\epsilon_2^1 = 1. \quad (\text{A.10})$$

A.2 Remarks on Fermions in Euclidean Space

We make some remarks on the relationship between fermions in Minkowski spacetime and Euclidean space. As an example, we consider the Lagrangian in Minkowski spacetime,

$$\mathcal{L}_M = (\chi_L)_{\dot{\alpha}}^{\dagger} i(\bar{\sigma}_M^{\mu})^{\dot{\alpha}\alpha} \partial_{\mu}(\chi_L)_{\alpha} + (\bar{\eta}_R)^{\alpha} i(\sigma_M^{\mu})_{\alpha\dot{\alpha}} \partial_{\mu}(\bar{\eta}_R)^{\dagger\dot{\alpha}} - m(\chi_L)_{\alpha}(\bar{\eta}_R)^{\alpha} - m(\chi_L)_{\dot{\alpha}}^{\dagger}(\bar{\eta}_R)^{\dagger\dot{\alpha}}. \quad (\text{A.11})$$

Here, both $(\chi_L)_{\alpha}$ and $(\bar{\eta}_R)^{\alpha}$ are left-handed Weyl spinors. We follow the conventions of the spinor indices in Minkowski spacetime in Ref. [55].

In Minkowski spacetime, χ_L^{\dagger} and $\bar{\eta}_R^{\dagger}$ are the hermitian conjugates of χ_L and $\bar{\eta}_R$. In Euclidean space, on the other hand, $(\chi_L^{\dagger}, \bar{\eta}_R^{\dagger})$ and $(\chi_L, \bar{\eta}_R)$ should be translated into independent fermions, respectively. We introduce the subscripts A and B to distinguish the dotted and undotted spinors in Euclidean space, which are related to the left-handed and right-handed Weyl fermions (i.e., undotted and the dotted fermions) in Minkowski spacetime via,

$$(\chi_L)_{\dot{\alpha}}^{\dagger} \rightarrow (\chi_A^{\dagger})_{\dot{\alpha}}, \quad (\chi_L)_{\alpha} \rightarrow (\chi_B)_{\alpha}, \quad (\bar{\eta}_R)^{\dagger\dot{\alpha}} \rightarrow (\bar{\eta}_A^{\dagger})^{\dot{\alpha}}, \quad (\bar{\eta}_R)^{\alpha} \rightarrow (\bar{\eta}_B)^{\alpha}. \quad (\text{A.12})$$

This notation is following Ref. [51]. In the main text, L/R , A/B and M/E subscripts are omitted since they should not cause any particular confusion.

Let us comment on this notation. In Euclidean space, the space rotation is $\text{SO}(4) \simeq \text{SU}(2)_A \times \text{SU}(2)_B$. The subscripts A or B of the fermions indicate which subgroup of spatial rotation is associated with the fermion, $\text{SU}(2)_A$ or $\text{SU}(2)_B$. Note again that fermions labeled with subscripts A and B are not related by Hermitian conjugation, and the \dagger symbol should be considered as part of the fermion's name rather than denoting a conjugate.

In this notation, the Minkowski Lagrangian (A.11) corresponds to the Euclidean Lagrangian,

$$\mathcal{L}_E = -(\chi_A^{\dagger})_{\dot{\alpha}} i(\bar{\sigma}_E^{\mu})^{\dot{\alpha}\alpha} \partial_{\mu}(\chi_B)_{\alpha} + (\bar{\eta}_B)^{\alpha} i(\sigma_E^{\mu})_{\alpha\dot{\alpha}} \partial_{\mu}(\bar{\eta}_A^{\dagger})^{\dot{\alpha}} - m(\chi_B)^{\alpha}(\bar{\eta}_B)_{\alpha} - m(\chi_A^{\dagger})_{\dot{\alpha}}(\bar{\eta}_A^{\dagger})^{\dot{\alpha}}. \quad (\text{A.13})$$

Here, raising and lowering indices α and $\dot{\alpha}$ are defined by multiplying the antisymmetric epsilon symbol as in Minkowski spacetime. An extra minus sign in front of $\bar{\sigma}_E$ is relevant to reproduce the Minkowski propagators by Wick rotation.

We use the following notation,

$$\bar{\not{D}}_E = -\bar{\sigma}_E^{\mu} \partial_{\mu}, \quad \not{D}_E = \sigma_E^{\mu} \partial_{\mu}, \quad (\text{A.14})$$

and also $\bar{\not{D}}_E$ and \not{D}_E for the covariant derivatives in gauge theories.

B Zero Modes of Massive Fermions around Constrained Instanton

We briefly summarize the features of fermion zero modes around the constrained instantons. As in Sec. 2.1, let us consider an $\text{SU}(2)$ gauge theory in Euclidean space. We introduce two pairs of $\text{SU}(2)$ singlet fermions $(\bar{e}_A^{\dagger}, \bar{e}_B)$ and $(\bar{\nu}_A^{\dagger}, \bar{\nu}_B)$, and a pair of $\text{SU}(2)$ doublet fermions $(\ell_A^{\dagger}, \ell_B)$. Note that each pair (f_A^{\dagger}, f_B) is mapped to f_L^{\dagger} and its conjugate f_L in Minkowski spacetime (see Eq. (A.12)). Here, following the notation in Ref. [51], the fermions are named like the SM leptons (and the right-handed neutrino), although they are not related to the SM leptons.

We consider the following Lagrangian,

$$\begin{aligned}
\mathcal{L}_E &= \frac{1}{2g^2} \text{Tr}(F_{\mu\nu}F_{\mu\nu}) + (D_\mu H)^\dagger(D_\mu H) + \frac{\lambda}{4}(H^\dagger H - v^2)^2 \\
&\quad - \ell_A^\dagger i\bar{\sigma}_\mu D_\mu \ell_B + \bar{e}_B i\sigma_\mu \partial_\mu \bar{e}_A^\dagger + \bar{\nu}_B i\sigma_\mu \partial_\mu \bar{\nu}_A^\dagger \\
&\quad - y_e \ell_A^\dagger H \bar{e}_A^\dagger - y_e \bar{e}_B H^\dagger \ell_B - y_\nu \ell_A^\dagger (\epsilon H)^\dagger \bar{\nu}_A^\dagger - y_\nu \bar{\nu}_B (\epsilon H) \ell_B ,
\end{aligned} \tag{B.1}$$

where $y_{e,\nu}$ denote the Yukawa coupling constants, and ϵ denotes the two-dimensional anti-symmetric invariant tensor with respect to SU(2) gauge group. At the vacuum, the scalar obtains a VEV, $H = (0, v)^T$, and all the fermions obtain masses, $m_e = y_e v$ and $m_\nu = y_\nu v$, respectively. The fermion kinetic terms can be rewritten as

$$\mathcal{L}_E^f = \Psi^\dagger i\hat{\mathcal{D}}_H \Psi , \quad \Psi^\dagger = \left(\ell_A^\dagger, \bar{e}_B, \bar{\nu}_B \right) , \quad \Psi = \begin{pmatrix} \ell_B \\ \bar{e}_A^\dagger \\ \bar{\nu}_A^\dagger \end{pmatrix} , \tag{B.2}$$

where we have defined the derivative operator,

$$i\hat{\mathcal{D}}_H \equiv \begin{pmatrix} -i\bar{\sigma}_\mu D_\mu^{\text{inst}} & -y_e H^{\text{inst}} & -y_\nu (\epsilon H^{\text{inst}})^\dagger \\ -y_e H^{\text{inst}\dagger} & i\sigma_\mu \partial_\mu & 0 \\ -y_\nu (\epsilon H^{\text{inst}}) & 0 & i\sigma_\mu \partial_\mu \end{pmatrix} . \tag{B.3}$$

Here, the superscript ‘‘inst’’ denotes the constrained instanton background (see Eqs. (2.4) and (2.5)). Note that the off-diagonal elements give the mass terms for the fermions at far from the instanton, i.e., $H^{\text{inst}}|_{x \rightarrow \infty} \rightarrow (0, v)^T$.

As discussed in Ref. [51], $i\hat{\mathcal{D}}_H$ has a normalizable zero mode in the anti-instanton background which behaves as

$$\ell_{B\alpha i}(x) = x_\mu (\sigma_\mu)_{\alpha\dot{\alpha}} \left[\mathcal{N} \frac{\rho}{x(x^2 + \rho^2)^{3/2}} \epsilon^{\dot{\alpha}i} + \mathcal{O}((\rho m_{A,H,e,\nu})^2) \right] , \tag{B.4}$$

$$\bar{e}_A^{\dagger\dot{\alpha}}(x) = -\frac{i}{2} \mathcal{N} \rho m_e \frac{1}{x^2 + \rho^2} \delta^{\dot{\alpha}1} + \mathcal{O}((\rho m_{A,H,e})^2) , \tag{B.5}$$

$$\bar{\nu}_A^{\dagger\dot{\alpha}}(x) = +\frac{i}{2} \mathcal{N} \rho m_\nu \frac{1}{x^2 + \rho^2} \delta^{\dot{\alpha}2} + \mathcal{O}((\rho m_{A,H,\nu})^2) , \tag{B.6}$$

at $x \ll m_{A,H,e,\nu}^{-1}$. They decay exponentially at $x \gg m_{A,H,e,\nu}^{-1}$. Here, i denotes the gauge SU(2) index of the doublet fermion, and \mathcal{N} is a finite normalization constant. In the instanton background, on the other hand, there are zero modes in ℓ_A^\dagger with $\mathcal{O}(\rho m_{e,\nu})$ contributions of e_B^\dagger and ν_B^\dagger . In Minkowski spacetime, the zero mode around the constrained anti-instanton appears in ℓ_L (with $\bar{e}_R^\dagger/\bar{\nu}_R^\dagger$) and the zero mode around the constrained instanton in ℓ_L^\dagger (with $\bar{e}_R/\bar{\nu}_R$).

References

- [1] R. D. Peccei and H. R. Quinn, Phys. Rev. Lett. **38**, 1440 (1977).

- [2] R. D. Peccei and H. R. Quinn, Phys. Rev. D **16**, 1791 (1977).
- [3] S. Weinberg, Phys. Rev. Lett. **40**, 223 (1978).
- [4] F. Wilczek, Phys. Rev. Lett. **40**, 279 (1978).
- [5] S. W. Hawking, Phys. Lett. B **195**, 337 (1987).
- [6] G. V. Lavrelashvili, V. A. Rubakov, and P. G. Tinyakov, JETP Lett. **46**, 167 (1987).
- [7] S. B. Giddings and A. Strominger, Nucl. Phys. B **307**, 854 (1988).
- [8] S. R. Coleman, Nucl. Phys. B **310**, 643 (1988).
- [9] G. Gilbert, Nucl. Phys. B **328**, 159 (1989).
- [10] T. Banks and N. Seiberg, Phys. Rev. D **83**, 084019 (2011), arXiv:1011.5120 [hep-th] .
- [11] M. Kamionkowski and J. March-Russell, Phys. Lett. B **282**, 137 (1992), arXiv:hep-th/9202003 .
- [12] R. Holman, S. D. H. Hsu, T. W. Kephart, E. W. Kolb, R. Watkins, and L. M. Widrow, Phys. Lett. B **282**, 132 (1992), arXiv:hep-ph/9203206 .
- [13] G. Lazarides and Q. Shafi, Phys. Lett. B **115**, 21 (1982).
- [14] S. M. Barr and D. Seckel, Phys. Rev. D **46**, 539 (1992).
- [15] A. G. Dias, V. Pleitez, and M. D. Tonasse, Phys. Rev. D **69**, 015007 (2004), arXiv:hep-ph/0210172 .
- [16] L. M. Carpenter, M. Dine, and G. Festuccia, Phys. Rev. D **80**, 125017 (2009), arXiv:0906.1273 [hep-th] .
- [17] G. Lazarides, C. Panagiotakopoulos, and Q. Shafi, Phys. Rev. Lett. **56**, 432 (1986).
- [18] K.-S. Choi, H. P. Nilles, S. Ramos-Sanchez, and P. K. S. Vaudrevange, Phys. Lett. B **675**, 381 (2009), arXiv:0902.3070 [hep-th] .
- [19] K. Harigaya, M. Ibe, K. Schmitz, and T. T. Yanagida, Phys. Rev. D **88**, 075022 (2013), arXiv:1308.1227 [hep-ph] .
- [20] T. Gherghetta, N. Nagata, and M. Shifman, Phys. Rev. D **93**, 115010 (2016), arXiv:1604.01127 [hep-ph] .
- [21] H. Fukuda, M. Ibe, M. Suzuki, and T. T. Yanagida, Phys. Lett. B **771**, 327 (2017), arXiv:1703.01112 [hep-ph] .
- [22] H. Fukuda, M. Ibe, M. Suzuki, and T. T. Yanagida, JHEP **07**, 128 (2018), arXiv:1803.00759 [hep-ph] .
- [23] M. Ibe, M. Suzuki, and T. T. Yanagida, JHEP **08**, 049 (2018), arXiv:1805.10029 [hep-ph] .

- [24] H.-C. Cheng and D. E. Kaplan, (2001), arXiv:hep-ph/0103346 .
- [25] K. I. Izawa, T. Watari, and T. Yanagida, Phys. Lett. B **534**, 93 (2002), arXiv:hep-ph/0202171 .
- [26] C. T. Hill and A. K. Leibovich, Phys. Rev. D **66**, 075010 (2002), arXiv:hep-ph/0205237 .
- [27] A. Fukunaga and K. I. Izawa, Phys. Lett. B **562**, 251 (2003), arXiv:hep-ph/0301273 .
- [28] K. I. Izawa, T. Watari, and T. Yanagida, Phys. Lett. B **589**, 141 (2004), arXiv:hep-ph/0403090 .
- [29] K.-w. Choi, Phys. Rev. Lett. **92**, 101602 (2004), arXiv:hep-ph/0308024 .
- [30] B. Grzadkowski and J. Wudka, Phys. Rev. D **77**, 096004 (2008), arXiv:0705.4307 [hep-ph] .
- [31] R. L. Workman and Others (Particle Data Group), PTEP **2022**, 083C01 (2022).
- [32] J. E. Kim, Phys. Rev. D **31**, 1733 (1985).
- [33] K. Choi and J. E. Kim, Phys. Rev. D **32**, 1828 (1985).
- [34] L. Randall, Phys. Lett. B **284**, 77 (1992).
- [35] B. A. Dobrescu, Phys. Rev. D **55**, 5826 (1997), arXiv:hep-ph/9609221 .
- [36] M. Redi and R. Sato, JHEP **05**, 104 (2016), arXiv:1602.05427 [hep-ph] .
- [37] B. Lillard and T. M. P. Tait, JHEP **11**, 005 (2017), arXiv:1707.04261 [hep-ph] .
- [38] B. Lillard and T. M. P. Tait, JHEP **11**, 199 (2018), arXiv:1811.03089 [hep-ph] .
- [39] M. B. Gavela, M. Ibe, P. Quilez, and T. T. Yanagida, Eur. Phys. J. C **79**, 542 (2019), arXiv:1812.08174 [hep-ph] .
- [40] L. Vecchi, Eur. Phys. J. C **81**, 938 (2021), arXiv:2106.15224 [hep-ph] .
- [41] R. Contino, A. Podo, and F. Revello, JHEP **04**, 180 (2022), arXiv:2112.09635 [hep-ph] .
- [42] P. Agrawal and K. Howe, JHEP **12**, 029 (2018), arXiv:1710.04213 [hep-ph] .
- [43] J. Fuentes-Martín, M. Reig, and A. Vicente, Phys. Rev. D **100**, 115028 (2019), arXiv:1907.02550 [hep-ph] .
- [44] C. Csáki, M. Ruhdorfer, and Y. Shirman, JHEP **04**, 031 (2020), arXiv:1912.02197 [hep-ph] .
- [45] T. Gherghetta, V. V. Khoze, A. Pomarol, and Y. Shirman, JHEP **03**, 063 (2020), arXiv:2001.05610 [hep-ph] .
- [46] R. Kitano and W. Yin, JHEP **07**, 078 (2021), arXiv:2103.08598 [hep-ph] .
- [47] C. Csáki, R. T. D’Agnolo, E. Kuflik, and M. Ruhdorfer, JHEP **04**, 074 (2024), arXiv:2311.09285 [hep-ph] .

- [48] R. Bedi, T. Gherghetta, C. Grojean, G. Guedes, J. Kley, and P. N. H. Vuong, (2024), arXiv:2402.09361 [hep-ph] .
- [49] H. Fukuda, K. Harigaya, M. Ibe, and T. T. Yanagida, Phys. Rev. D **92**, 015021 (2015), arXiv:1504.06084 [hep-ph] .
- [50] I. Affleck, Nucl. Phys. B **191**, 429 (1981).
- [51] O. Espinosa, Nucl. Phys. B **343**, 310 (1990).
- [52] C. Csaki and H. Murayama, Nucl. Phys. B **532**, 498 (1998), arXiv:hep-th/9804061 .
- [53] G. 't Hooft, Phys. Rev. D **14**, 3432 (1976), [Erratum: Phys.Rev.D 18, 2199 (1978)].
- [54] G. 't Hooft, Phys. Rev. Lett. **37**, 8 (1976).
- [55] H. K. Dreiner, H. E. Haber, and S. P. Martin, Phys. Rept. **494**, 1 (2010), arXiv:0812.1594 [hep-ph] .